Shelf Life Study of Electrospun PLGA Copolymers

California Polytechnic State University, San Luis Obispo

Senior Project

Sean Youra

Nick Hudson

Advisor: Dr. Kristen O'Halloran Cardinal

Submitted: June 2013

Abstract

Poly(lactic-co-glycolic acid) (PLGA) is one of the most commonly used copolymers for electrospinning in tissue engineering applications. However, most research has not focused on the copolymer itself in regards to how long it can be used effectively and if varying the concentrations of polylactic acid (PLA) and polyglycolic acid (PGA) affect the resulting properties. Electrospinning is the method we use to create the three-dimensional constructs, or “scaffolds”, for the blood vessel mimic (BVM) in the tissue engineering lab. The aim of our project was to investigate if the morphology and mechanical properties of the scaffolds changed over time when they were stored in a dessicator. In addition, the morphology and properties from 75:25 and 85:15 PLGA copolymers were studied to determine whether there were significant differences in fiber diameter, elastic modulus, or critical yield strength between them via Scanning Electron Microscopy (SEM) image analysis and tensile testing of the samples. These same three parameters were analyzed for the distal, medial, and proximal regions of the scaffold for each concentration of PLGA. The main significant finding was that the regions of the scaffold were relatively uniform in their properties. No timepoints were established, since there was such large variation in the data and the trends were inconsistent. A larger and longer duration study is needed to determine whether there is an ideal timeframe to use the scaffolds.

Acknowledgements

We would like to thank the following people for helping to contribute to our work:

First and foremost, Dr. Kristen Cardinal for being a terrific and very supportive senior project advisor throughout the whole process. Thank you for letting us use the tissue engineering lab for our research and for making sure we had everything we needed to finish the project in a timely manner. You were paramount to our success;

The Hannah Forbes Foundation, for funding some of our research. We would not have been able to complete our project without your gracious support;

Aubrey Dyer, for providing the initial Visual Basic macro that we used for the tensile testing procedure;

Dr. Lanny Griffin, for helping us modify the macro to suit our testing procedure;

Dr. Lily Laiho, for granting us permission to use the SEM for our research;

Mr. Laiho, for ordering any extra materials or supplies we needed;

Deven Patel and Shane Tipton, for teaching us the masterful ways of electrospinning;

All of the tissue engineering lab folks, including Stephan, Corey, Jakub, Alex, Scott, Mike, Rachel, and Sarah, for all your moral support , constructive criticism, and comradery;

And finally, we would like to thank our parents and close relatives for all their love and support. We would certainly not have gotten this far without you all.

Table of Contents

I. Introduction

Cardiovascular Disease

Cardiovascular diseases are the biggest cause of death worldwide [23]. In the United States alone, half a million people die of heart disease every year [23]. The most common cardiovascular disease is atherosclerosis, or a condition in which an artery wall thickens due to buildup of plaque. Plaque mainly consists of calcium, fibrous tissue, cholesterol, and fats. Specifically, when low-density lipoproteins (LDLs) accumulate in the blood as a result of deficient LDL receptors, this causes hypercholesterolemia. These LDLs are oxidized and are accumulated by macrophages, which then become foam cells. As a part of this immune response, cytokines are released that allow for the proliferation of smooth muscle cells into the intima of the artery, causing intimal thickening or atheroma. Over time, this changes the properties and physical appearance of the artery (Figure 1). The walls of the artery begin to harden and blood flow is impeded as the condition worsens.

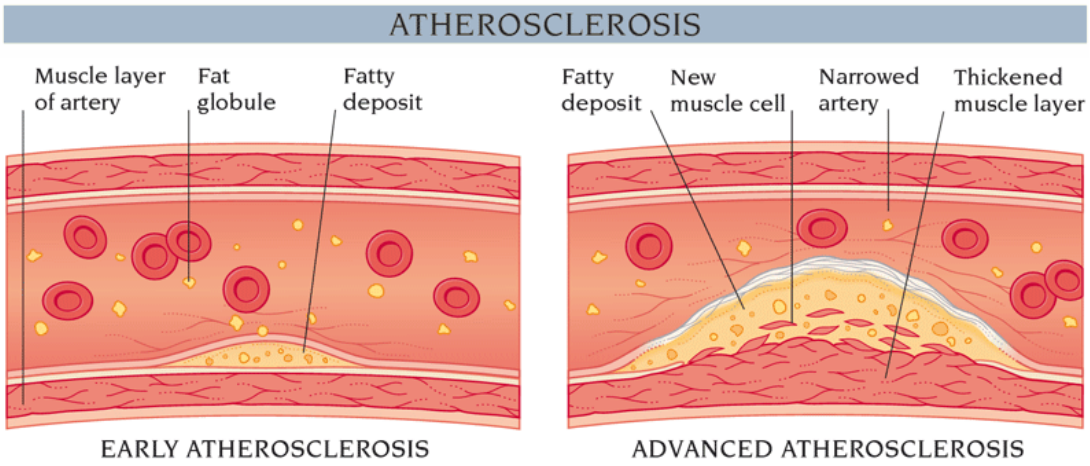

Figure 1: The progression of atherosclerosis from its early stages with increased plaque buildup to more advanced stages that include proliferation of smooth muscle into the intima, thickening of the vessel wall, and narrowing of the artery itself [1]

If exacerbated, this can cause thrombus formation and eventually lead to a myocardial infarction (MI) or stroke if the thrombus breaks off and becomes an embolus. Both a MI and stroke will

significantly shorten the lifespan of the individual, if it does not kill them in the process. Stroke also happens to be the third most common cause of death in the U.S.; cancer is second [3].

In addition, there are a number of atherosclerotic-related diseases such as coronary heart disease (CHD), carotid heart disease, peripheral artery disease, and chronic kidney disease, each affecting a different region of the vasculature. For example, CHD occurs when there is plaque build-up in the coronary arteries of the heart. Not surprisingly, it is also the most prominent cause of death among men and women in the United States, accounting for approximately one-third of all deaths [2, 3]. If ischemia occurs in the region, then a common symptom will be angina, or chest pain, which can be a warning sign for a potential MI. There are a number of risk factors associated with atherosclerosis including lack of exercise, poor nutrition, smoking, hypertension, diabetes, obesity, and a family history of heart disease [3].

Treatments

Current treatments for atherosclerosis include the use of drugs, surgical intervention, and lifestyle changes. Often times, lifestyle changes such as eating healthy are the best treatment for atherosclerosis [4]. Certain drugs, such as cholesterol medication, beta blockers, and calcium channel blockers can slow the effects of atherosclerosis. As atherosclerosis becomes worse, blockage of the artery can starve muscle and skin tissue of oxygen. At this point, a more aggressive procedure is needed to restore blood to the tissue. Some of the more common methods of surgical intervention are angioplasty and stent placement, endarterectomy, and bypass surgery. Coronary artery bypass surgery is one of the most common surgeries performed in the United States. Many advances in this surgery have lead to a minimally invasive method of grafting the bypass tissue even while the heart is still beating [5]. With a more minimally invasive surgery, recovery time and risk of infection decrease dramatically. The vessel graft in

the place of the artery comes from a different place in the body, commonly the greater saphenous veins. The graft vessel acts as a bypass so that blood can flow around the blockage (Figure 2).

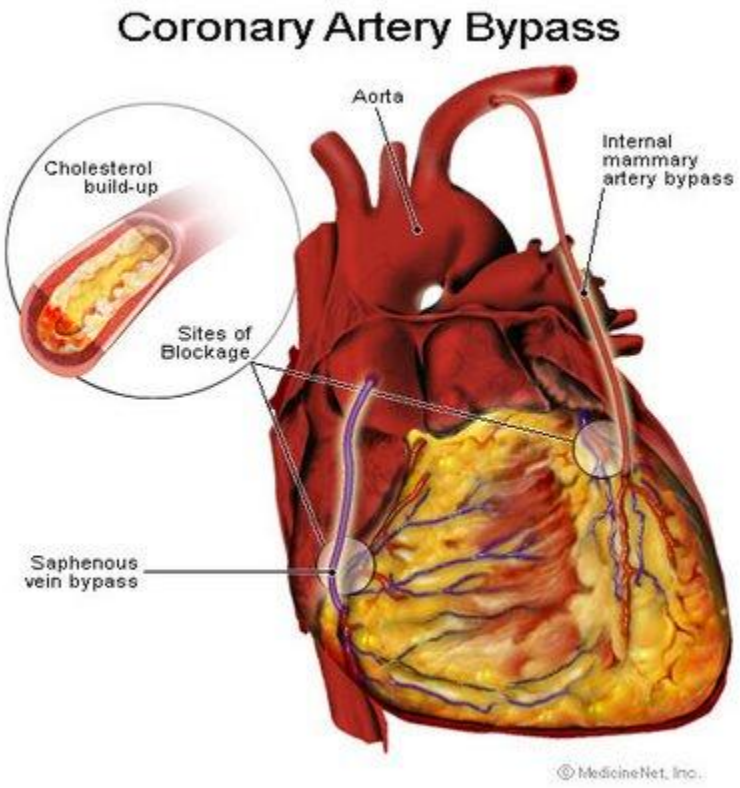

Figure 2: The sites of plaque buildup are shown within the coronary arteries. The artery bypass circumvents these occluded areas and allows blood to flow throughout the heart unhindered [6]

Tissue Engineering

In an attempt to provide a more permanent solution, a newly emerging field in biomedical engineering called tissue engineering offers promise for treating, and in certain cases, curing cardiovascular disease. It has been defined as “an interdisciplinary field that applies the principles of engineering and life sciences toward the development of biological substitutes that restore, maintain, or improve tissue function or a whole organ" [7]. Using either biological or artificial tissues, a construct or scaffold is created by various means including nanofiber self-assembly, solvent casting and particulate leaching, gas foaming, emulsification, or

electrospinning, among others [8]. Cells are then "seeded" or implanted into the scaffold using a bioreactor set-up; see Figure 3. The bioreactor provides a similar environment to the cells' natural physiological environment, which allows them to grow and proliferate. The basic process of creating tissue scaffolds from initial polymer processing and cell seeding to various applications it can be used for is shown in Figure 4.

Figure 3: Bioreactor setup in the Cal Poly tissue engineering lab, including cell media reservoir (left), peristaltic pump system (middle), and perfused scaffolds housed in the bioreactors (right) [9]

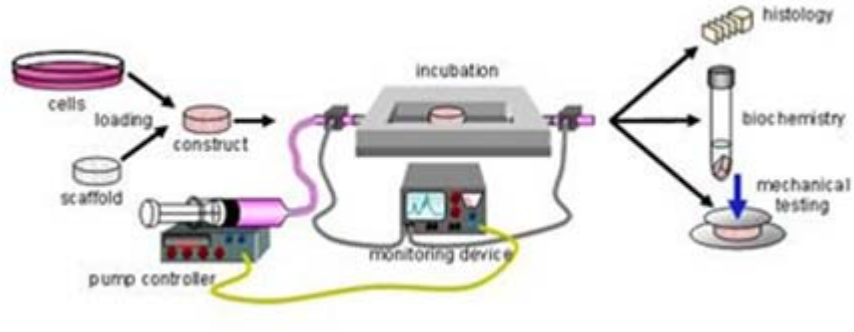

Figure 4: Process for Creating Tissue-engineered Scaffolds [10]

There are many important features that a scaffold must have in order to allow for maximal cell survival, which is usually measured in terms of confluency. These features include: high porosity, adequate pore size, biodegradability, and strong mechanical properties similar to

that of the native vessel or tissue. An advantage of using these artificially-grown tissues, vessels, and organs is that there would be no risk of rejection, since the patient's own cells would be used to create it. It also limits the amount of cells that are needed by the patient. Cell lines can be established by starting with a single cell line that can then grow and proliferate, with the correct growth and differentiation factors added, to create new cell lines. This would also be a very promising alternative to invasive surgeries, expensive grafts, and long waiting times for donor organs.

Originally used for degradable sutures, poly lactic-*co*-glycolic acid (PLGA) has been among the most attractive polymeric candidates used to fabricate devices for drug delivery and tissue engineering applications [24]. It has a controllable degradation rate, based on the compositions of PLA to PGA, and degrades via hydrolysis. The degradation products are not harmful and are eventually removed from the body as carbon dioxide and water [16]. Since all PLGAs are amorphous, the glass transition temperature and melting temperature are significantly higher than other polymers, especially as the amount of PGA increases [17]. All these properties of the copolymer are very important as they are most conducive to creating a vascular graft that has a controllable degradation rate, is biocompatible and will not harm the host, and has a glass transition temperature and melting temperature above normal body temperature. It also happens to be very soluble and relatively easy to process based on research done previously in the Cal Poly tissue engineering lab.

Electrospinning

The process of electrospinning will be looked at in more depth as it is the focus of our research. The main reason why electrospinning is more attractive than some of the other tissue engineering methods currently out there is it allows for the creation of non-woven polymeric

fibers on the nanoscale level. This, in turn, creates a very large surface area-to-volume ratio, which allows for maximum cell proliferation and attachment. The flexibility of the material along with its mechanical properties are markedly improved compared to at the micrometer level [11]. When cells are seeded into electrospun nanofibrous scaffolds, a greater quantity of extracellular matrix is produced than those seeded on microfibrous scaffolds. High porosity, improved mechanical properties, and morphological similarities to components of the native extracellular matrix allow for a greater degree of cell adhesion, cell proliferation, and mechanical integrity of the scaffold [12].Electrospinning seems to be one of the few processes that might have mass production potential as well, especially with new advances in multi-jet electrospinning and "blowing-assisted" electrospinning [13]. This is extremely important if tissue engineering is to go beyond the research stages and into clinical applications.

Before electrospinning, there was electrospraying, which was first described by Sir William Gilbert in the late 1500s. In his research, he observed how electrically charged amber would form a cone shape when placed near water, which would then "spray" droplets of amber from the tip of the cone. This cone shape was later named a "Taylor cone" after Sir Geoffrey Ingram Taylor who mathematically modeled the shape of this cone as a result of the electric field that was created [14]. Recent work has focused on using organic and synthetic polymers as the feedstock, as it is typically called, for a range of applications including tissue engineering, cosmetics, composite reinforcement, protective clothing, and electronics [15].

In order to create a scaffold through the process of electrospinning, the polymer must first be dissolved in a solvent such as chloroform. It must then be charged using a high voltage power supply (in the kV range) by attaching the positive electrode to the syringe that contains the solution. A ground electrode attached to the collector system is needed to effectively allow the

polymer to travel from the syringe to the mandrel attached to the collector. As the charge builds up within the solution, the solution's hemispherical shape begins to elongate forming the Taylor cone at the tip of the syringe. Eventually, the normal effects of surface tension are overcome by electrostatic repulsive forces. At this point, the fluid ejects from the tip of the syringe and begins a complicated whipping instability pattern, which is pictured below in Figure 5. This whipping pattern results from perturbations in the motion and trajectory of the fiber jet that overcome the viscoelastic nature of the polymer [14,18]. This phenomenon is very important to the entire process, however, as it allows most of the solvent to evaporate leaving behind just the polymer. It also allows the fiber to further elongate and form a nanofibrous matrix on the mandrel. A simplified setup of the electrospinning process is shown in Figure 6.

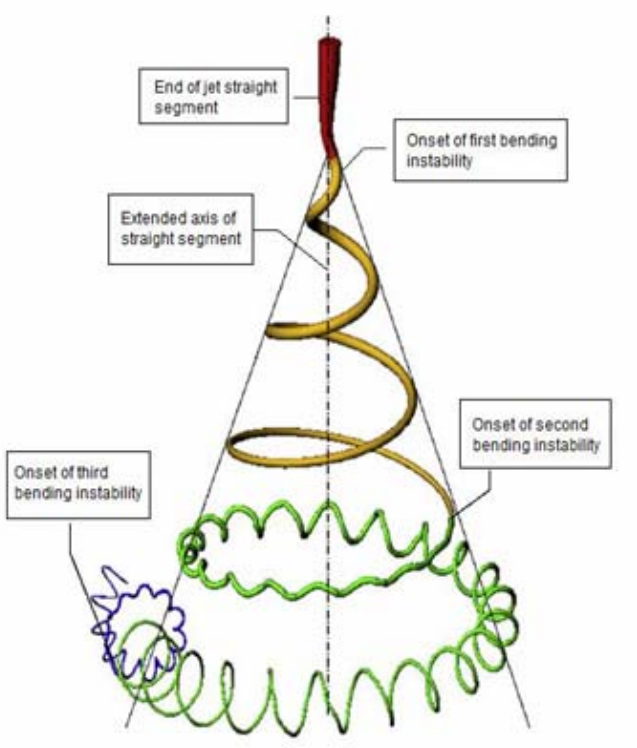

Figure 5: Diagram of the whipping instability that occurs during the ejection of the solution from the syringe [19]

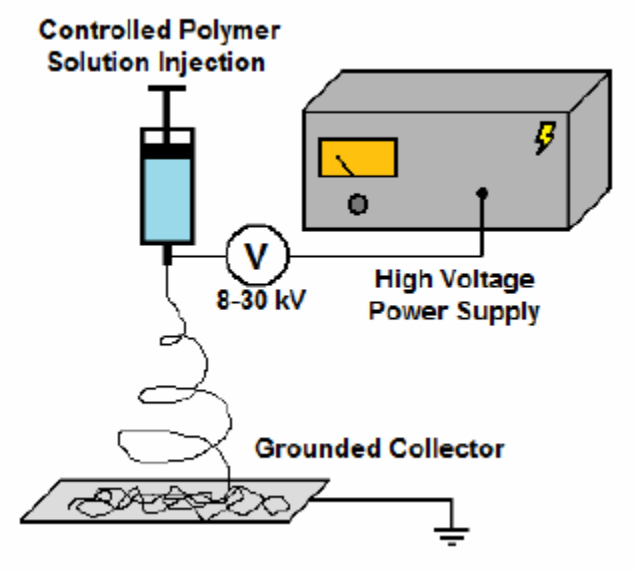

Figure 6: Basic setup for electrospinning that includes the power supply, syringe, and collector system [19]

There are a number of parameters to consider that will affect the resulting scaffold that is created via the electrospinning process. These parameters include the voltage of the power supply, gap distance between the mandrel and syringe, feedrate of the polymer, and both the rotational and translational movement of the grounded mandrel. The magnitude of the voltage supply is an important parameter because it controls the fiber diameter and fiber orientation of the fibers in the scaffold. The voltage of the power supply determines the velocity of the polymer jet. The higher the voltage, the faster the polymer travels and the less time the polymer has before it is collected at the mandrel. This is called the flight time of the polymer [20]. Due the behavior of the polymer inside the Taylor cone, higher voltages result in less flight time, which allows for less elongation of the fiber and less whipping instability to occur. If the voltage is too low compared to the extrusion rate, polymer will fall into the collecting tray. On the other hand, if the voltage is too high, the fiber diameter will become inconsistent. This phenomenon is called

"beading." The gap distance between the syringe and the mandrel not only allows the solvent to evaporate, but also plays a role in fiber orientation and diameter [11].

Previous Electrospinning Work

Although there has been a fair amount of research into how changing the various parameters of the electrospinning setup can affect the scaffold properties, very little research has focused on how time and different environments can affect these properties. Although relative degradation rates are known for many of the synthetic polymers used in electrospinning research [13], it would be worthwhile to determine a timeframe in which the scaffold itself is most viable for cell attachment and growth. Since the scaffold is placed within a bioreactor setup after drying within a dessicator and is subjected to fluid flow, the properties are bound to change compared to when it is in a dry environment. In addition, the mechanical properties and fiber morphology between different concentrations of PLGA has not been given much attention. The modulus for different concentrations of PLGA has been documented, but in their unprocessed form [13]. Thus, mechanical properties after electrospinning have yet to be published and are bound to be subject to the preparation of the solution and specific parameters used for the electrospinning setup. It is important to find synthetic polymer that most closely resembles the native vasculature in terms of its mechanical properties, hence why changing the concentrations of PLA and PGA may be beneficial to achieve such properties.

Electrospinning work prior to this project has looked at setting up a working electrospinner for in-house fabrication of our Blood Vessel Mimic (BVM) model by Colby James [19], and the preparation and characterization of the electrospun PLGA scaffolds by Tiffany Peña [25]. Additionally, the parameters for the current electrospinner were optimized by

Deven Patel for the Blood Brain Barrier setup [26]. Achieving consistent fiber morphology that is conducive to greater cell adhesion and proliferation is important to the overall goal of our lab.

Summary and Goals

The aim of our project is to investigate if the morphology and mechanical properties of the scaffolds change over time when they are stored in the dessicator. If they do change with time, then timepoints will need to be established to mark any significant changes. For example, if there is a significant decrease in modulus after 14 days in the dessicator, then this can be documented so that way others conducting blood vessel mimic (BVM) research know when to use them by. This will ensure that their research stays consistent and is not affected by changes in fiber morphology or mechanical properties. In addition, the morphology and mechanical properties from 75:25 and 85:15 PLGA copolymers will be characterized and documented to determine whether there are significant differences in fiber diameter, elastic modulus, or critical yield strength among them. If consistent mechanical properties and fiber morphology are exhibited by one of the other copolymer concentrations in terms of the application, then further research may be warranted into their use in BVMs. These same parameters will be analyzed for various regions of the scaffold to ensure properties are uniform throughout.

II. Methods

Polymer Mixing

A copolymer of Poly(lactic-co-glycolic acid), or PLGA, with separate compositions of lactic acid and glycolic acid, were obtained from Sigma Aldrich (Milwaukee, WI). PLGA 85:15 has a composition of eighty-five percent lactic acid to fifteen percent glycolic acid, and PLGA 75:25 consist of seventy-five percent lactic acid with twenty-five percent glycolic acid. The copolymer was dissolved in chloroform ($CHCl_3$) to create a 15 wt% polymer (WPP) solution in

accordance to the protocol specified in Appendix A1. Four vials of 75:25 and four vials of 85:15, each with three milliliters of chloroform, were used. Polymer pellets were carefully weighed out to 0.7835 grams and chloroform was measured out to 3 milliliters for each solution in order to achieve consistent WPP solution, according to Appendix A1. An orbital mixing table was used to mix the polymer solution for twenty-four hours. After the polymer mixed for twenty-four hours, the solution was viable for forty-eight hours.

Electrospinning

Parameters used in the electrospinning process can be seen in Table 1 below. Additionally, the settings of the electrospinning device were set to the following: translational speed set to 3 (55 OPM), translational distance set to 16 cm, and rotational speed set to 6 (3110 RPM).

Table 1: List of parameters used for electrospinning

Voltage	-12000 Volts (negative polarity)
Flow Rate	5.5 mL/hr
Gap Distance	10 inches
Needle Size	18 gauge, beveled blunt (BD 305180)

**Note: Based on a previous study that we conducted in our lab, it was found that -12.5 kV was more ideal for 85:15 PLGA in terms of fiber consistency and properties, so this voltage was used when electrospinning the 85:15 (See appendix A4 for a summary of this study).*

After mixing was completed and twenty-four hours passed, both solutions were electrospun to create a total of eight scaffolds. Electrospinning was carried out according to the

electrospinning protocol laid out by Deven Patel which was modified for this particular study (Appendix A2). In order to allow the solvent to fully evaporate from the scaffold, all the scaffolds were stored in the dessicator for twenty-four hours. After this latent period, scaffolds were cut into sections for testing. Testing section dimensions can be seen in Figure 7. Scaffolds were sectioned using a carbon steel blade into proximal, medial, and distal sections. These sections were then cut into smaller half centimeter by one centimeter pieces for testing and placed in multiple 12 well plates that were labeled with each test day, sample type, and sample location.

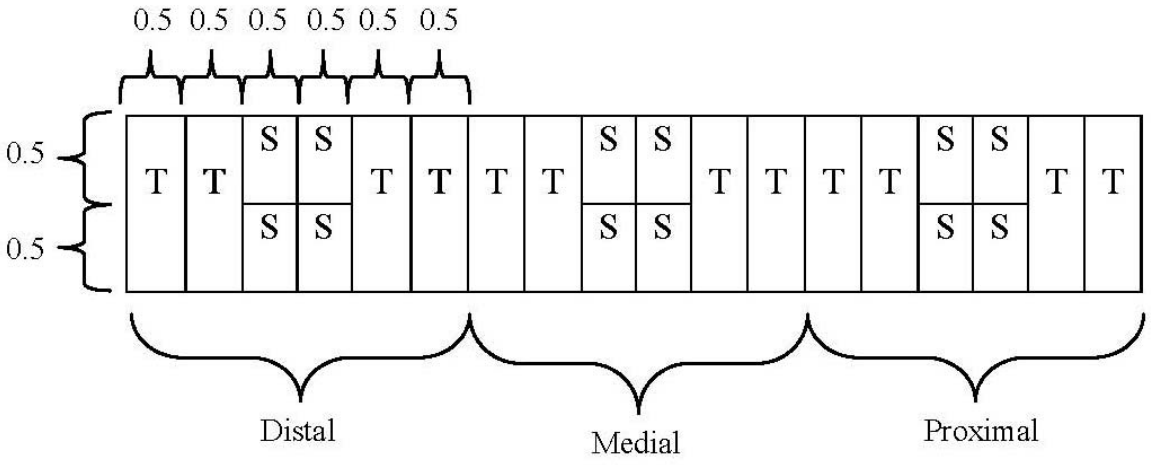

Figure 7: Section dimensions (in centimeters) and labels for each scaffold. Dimensions are repeated for medial and proximal regions (not shown). T signifies a tensile testing sample, where S signifies a SEM sample

SEM Sample Preparation

In order to properly view the samples with the SEM, they had to be dehydrated first. The dehydration protocol is as follows: 5 minutes in distilled H_2O, 5 minutes in 25% EtOH, 5 minutes in 50% EtOH, 5 minutes in 70% EtOH, 5 minutes in 95% EtOH, 5 minutes in 100% EtOH, 5 minutes in 100% EtOH. The samples were transferred into the labeled vials of EtOH

with tweezers. Each sample was dehydrated in the same manner twenty-four prior to SEM analysis. The samples were placed back into their respective well plates after dehydration.

SEM and Image Analysis

The inner lumen of each sample section was imaged at random locations at 500x magnification using a Hitachi TM-1000 tabletop SEM. Only one image per sample was taken. First, the specimen stage was pulled out of the SEM and placed in the specimen height gage. A small piece of double-sided non-conducting tape was applied to the specimen stage to ensure the samples would be held down properly. Each sample from a particular region was placed with tweezers onto the stage, so that four samples would be imaged in a single set-up in the essence of time. After the samples had been placed on the stage, the height gage was used to ensure there was at least 1 mm of clearance, so that the samples would not be disturbed when inserting them into the SEM. A laptop was hooked up the SEM, which had the proper software for the TM-1000. By pressing the evacuation button on the SEM, the chamber was evacuated to allow for clearer viewing of the sample. Each sample was carefully tracked by starting from the top of the stage and imaging each sample going down using the translational knobs on the SEM. After obtaining the correct magnification and focusing the image, the image was saved for later analysis in ImageJ. The evacuation button was pressed again after viewing all the samples for a certain region and a new sample set for another region was loaded onto the stage for imaging. A single image was taken for each of the SEM samples after verifying that the image taken was representative of the sample. Images taken did not include any edges of the sample since fiber morphology would be more likely to be affected there from cutting the sample. This was repeated for both concentrations over the course of the study. Fibers were measured using a measuring macro in ImageJ. Line segments were manually moved onto the edges of each fiber.

The line segments used for measuring showed the number of pixels in each line segment. By measuring the fiber diameter and a given length bar at the bottom of the image, a value for the fiber diameter was calculated. For each image, fibers were chosen at random from six circles made on every image. Fiber diameter data is the average length of the six representative fibers.

Tensile Testing and Stress Strain Analysis

Samples of scaffold designated for tensile testing were tested at various timepoints in order to represent the mechanical properties of the electrospun polymer over time. A testing schedule was created and timepoints for data sampling were set every seven days. Tensile testing samples were tested to failure using the Instron InSpec 2200 Tensile Testing Machine on campus. A PalmPilot PDA was used as a data acquisition unit to record data in a time, extension, and load format. The load was zeroed by pressing the "bal" button on the data acquisition unit before testing each day to ensure a consistent baseline reading for the load. Initial dimensions of samples were measured and recorded with calipers. The gauge length of the sample was measured after the sample was placed in the tensile tester and clamped into place. The gauge length of the sample is defined as the distance between the clamps of the tensile tester. Samples were clamped into place using the hand screws on the test fixture. The extension was zeroed before each sample test to eliminate a negative reading for the extension. This was done because the macro we use cannot read data with negative extensions in the data set. Samples were pulled in tension until a 0.5 N change in the load occurred. The tensile testing machine was switched to its testing state which pulls samples at a consistent rate of 20 mm/min. Data output from the Instron InSpec 2200 Tensile Tester was converted to data compatible with Microsoft Excel. By modifying an existing macro in Visual Basic, given to us by Aubrey Dyer, stress versus strain

curves were generated for all of our tensile testing samples. This macro is located in Appendix A3.

Statistical Analysis

Two-sample t-tests were performed to compare sample concentrations, sample regions, and samples that were tested on different days using Minitab 16 (2010). A p-value of 0.05 was used for statistical significance. The timepoints that were compared were day 1, 7, 14, 21, and 28.

III. Results

SEM and Image Analysis

Following the protocol specified in the methods section, SEM images were taken for all samples for each region and concentration for the particular day of testing. In order to expedite the imaging process, the four samples from a particular region e.g. distal were all placed on the specimen stage instead of imaging each sample one by one. All images were taken at 500x magnification as specified in the methods section. Representative images for the two concentrations, 75:25 and 85:15 PLGA, are shown below in figures 8 and 9.

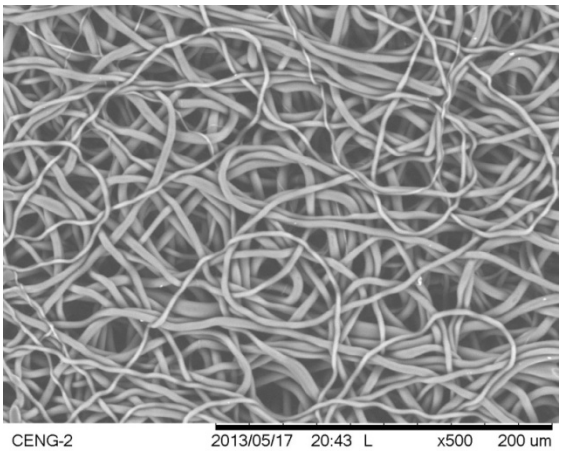

Figure 8: Representative SEM image for 75:25 PLGA, taken from the distal region on day 28 of testing

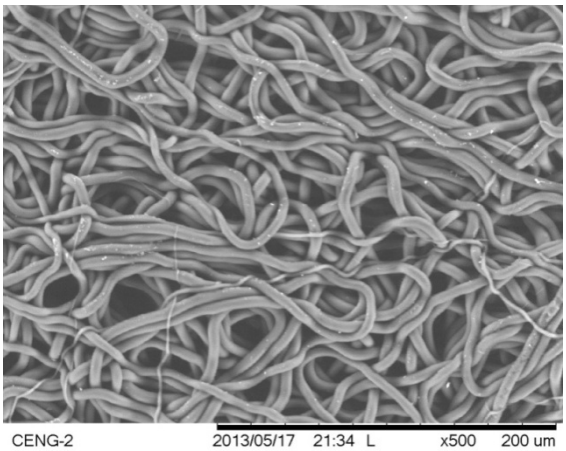

Figure 9: Representative SEM image for 85:15 PLGA, taken from the distal region on day 28 of testing

Important things to note about the images include the relative porosities, alignment of the fibers, thickness of the fibers, and overall consistency of the fibers. After all images had been taken for a particular day of testing, 6 fibers were analyzed in ImageJ for each image and an average was taken. Average fiber diameters for the various regions of 75:25 and 85:15 PLGA over the course of the study can be seen in figures 10 and 11, respectively.

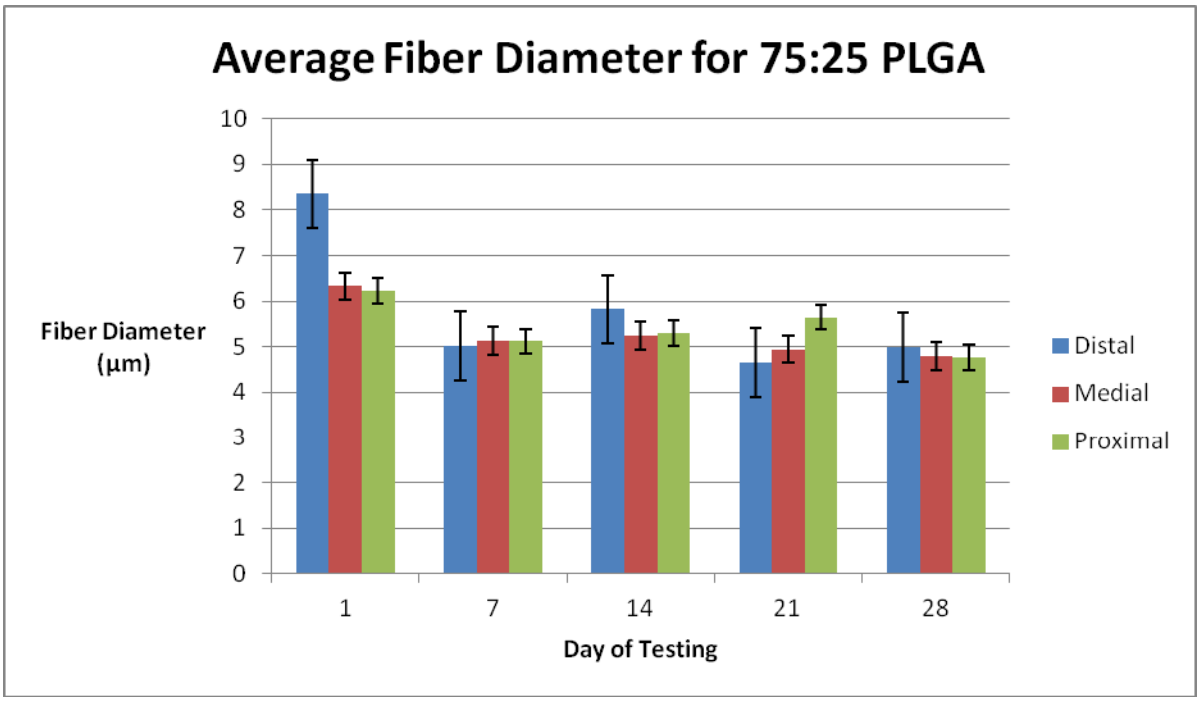

Figure 10: Average fiber diameter for 75:25 PLGA for the distal, medial, and proximal regions of the scaffold over the course of 28 days; n = 4

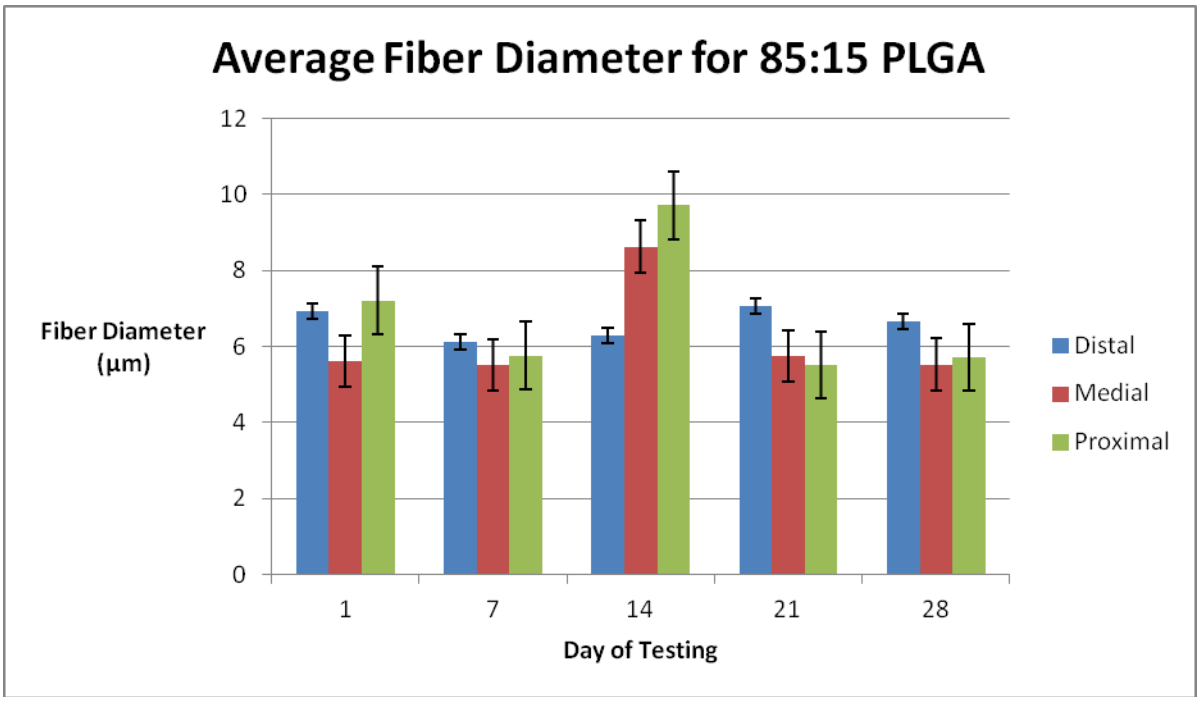

Figure 11: Average fiber diameter for 85:15 PLGA for the distal, medial, and proximal regions of the scaffold over the course of 28 days; n = 4

When performing two-sample t-tests in Minitab, no statistical differences were found among the regions and the different days of testing for both concentrations in terms of fiber diameter. Also, no visible trends can be seen for either figure 10 or 11.

Tensile Testing and Stress Strain Analysis

Tensile testing was performed as laid out in the methods section and stress-strain curves were outputted using the macro found in appendix A3. Representative stress-strain curves for 75:25 and 85:15 PLGA are shown in figures 12 and 13 below.

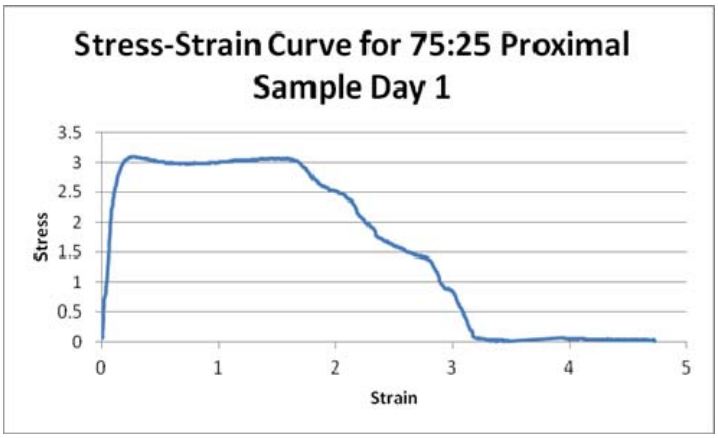

Figure 12: Representative stress-strain curve for 75:25 PLGA, taken from the proximal region on day 1 of testing

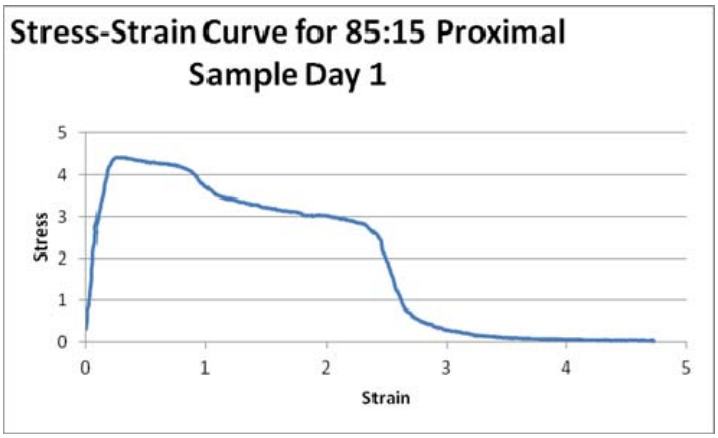

Figure 13: Representative stress-strain curve for 85:15 PLGA, taken from the proximal region on day 1 of testing

The linear portion of the stress-strain curve was also outputted simultaneously and the equation of the line provided the elastic modulus of the sample. In Excel, the ultimate tensile strength (UTS) was found from the maximum stress point along the curve and this was displayed as well. Average elastic modulus for the various regions of 75:25 and 85:15 PLGA over the course of the study can be seen in figures 14 and 15, respectively. Average UTS for the various regions of 75:25 and 85:15 PLGA over the course of the study can be seen in figures 16 and 17, respectively.

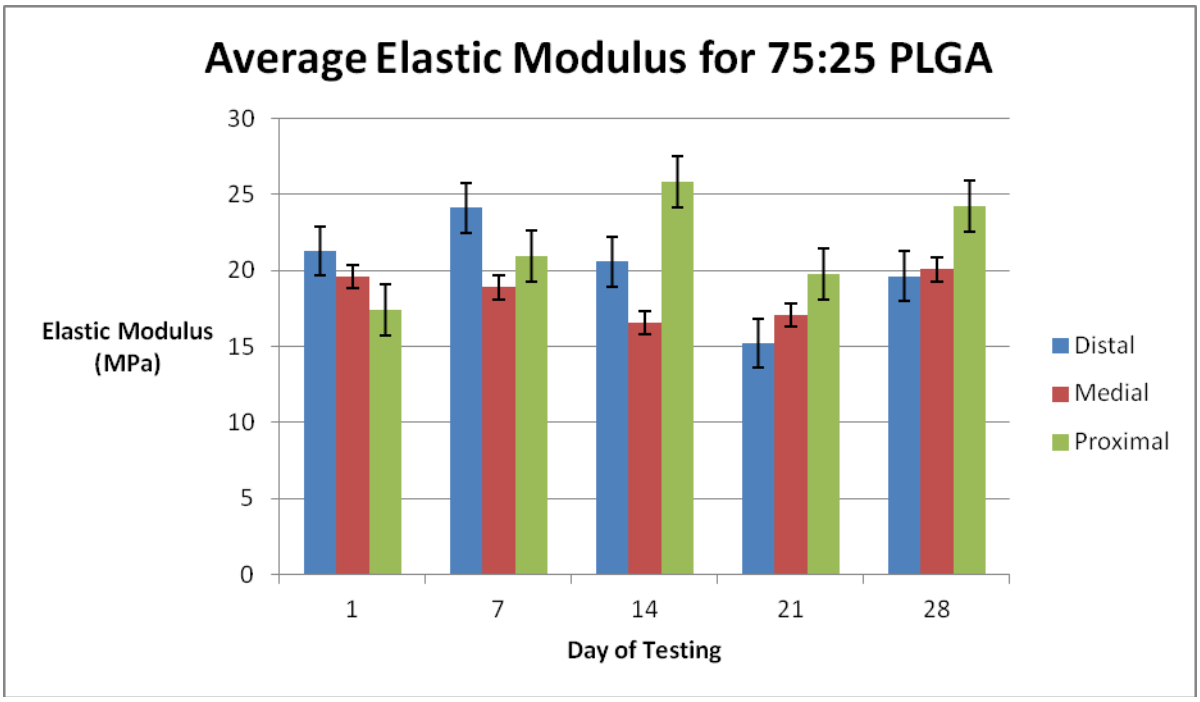

Figure 14: Average elastic modulus for 75:25 PLGA for the distal, medial, and proximal regions of the scaffold over the course of 28 days; n = 4

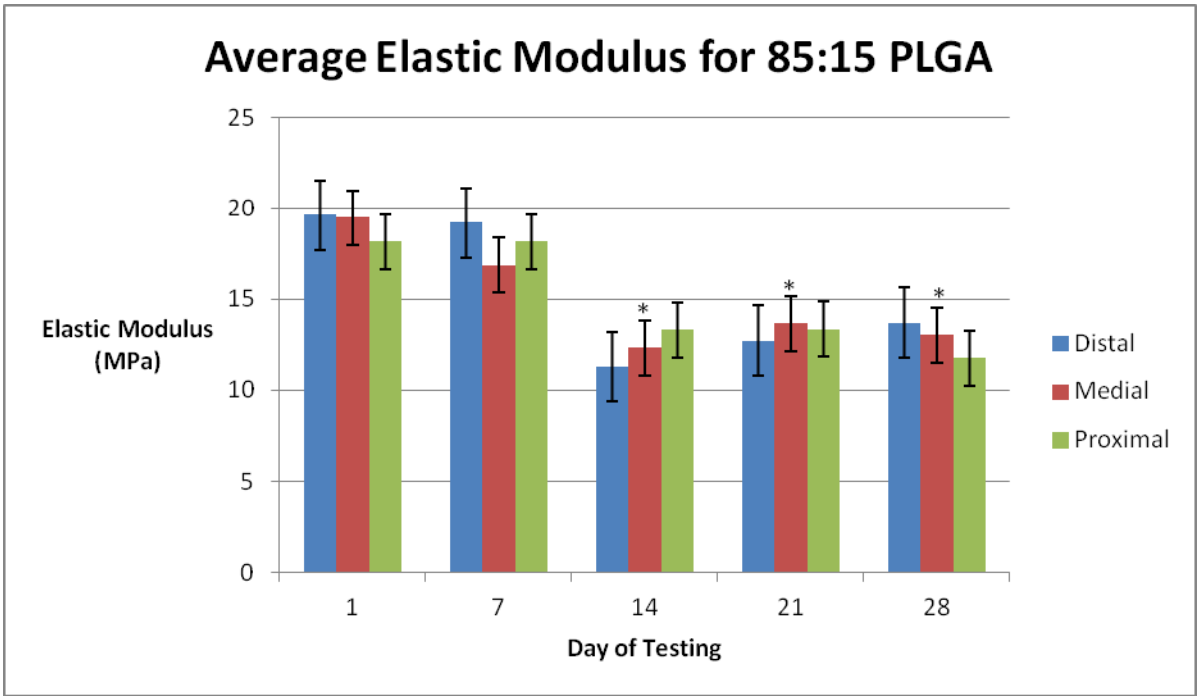

Figure 15: Average elastic modulus for 85:15 PLGA for the distal, medial, and proximal regions of the scaffold over the course of 28 days; n = 4; *, $p < 0.05$ versus day 1

When performing two-sample t-tests in Minitab, no statistical differences were found among the regions and the different days of testing for 75:25 PLGA in terms of elastic modulus. Also, no visible trend can be seen for figure 14. Conversely, for 85:15 PLGA, the modulus decreased significantly in the medial region for days 14, 21, and 28 compared to day 1. Similar trends can be seen for the distal and proximal regions when comparing days 14, 21, and 28 to day 1 in figure 15.

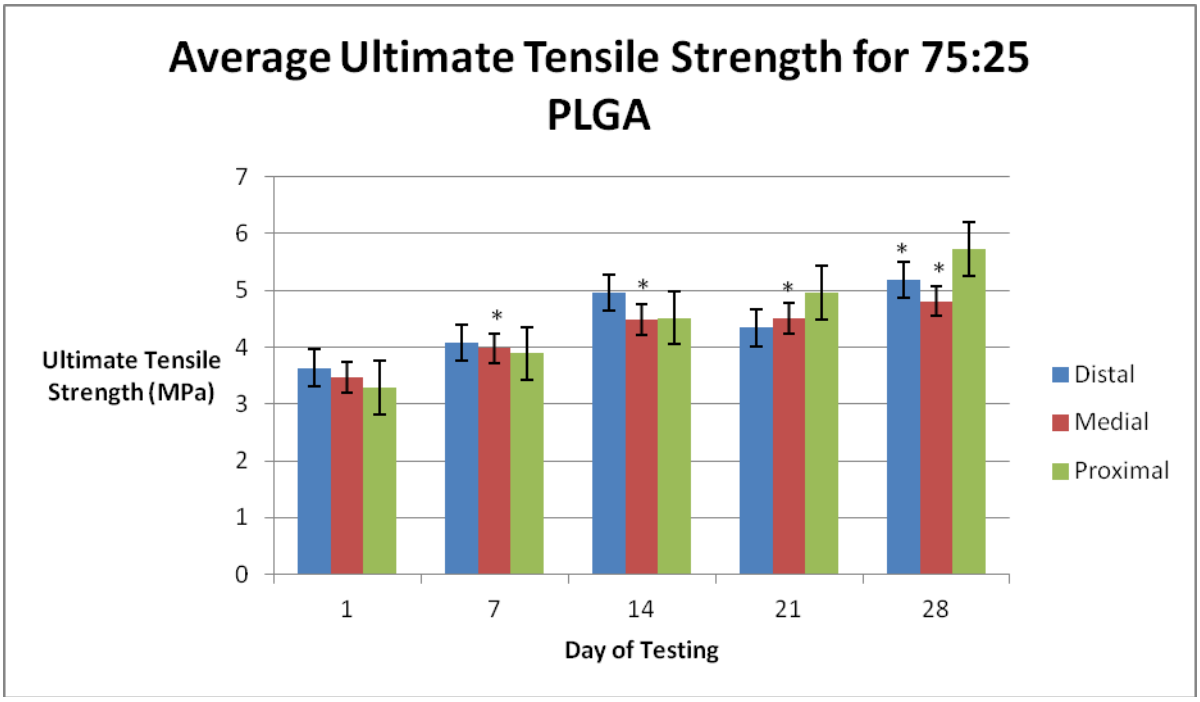

Figure 16: Average ultimate tensile strength for 75:25 PLGA for the distal, medial, and proximal regions of the scaffold over the course of 28 days; n = 4; *, $p < 0.05$ versus day 1

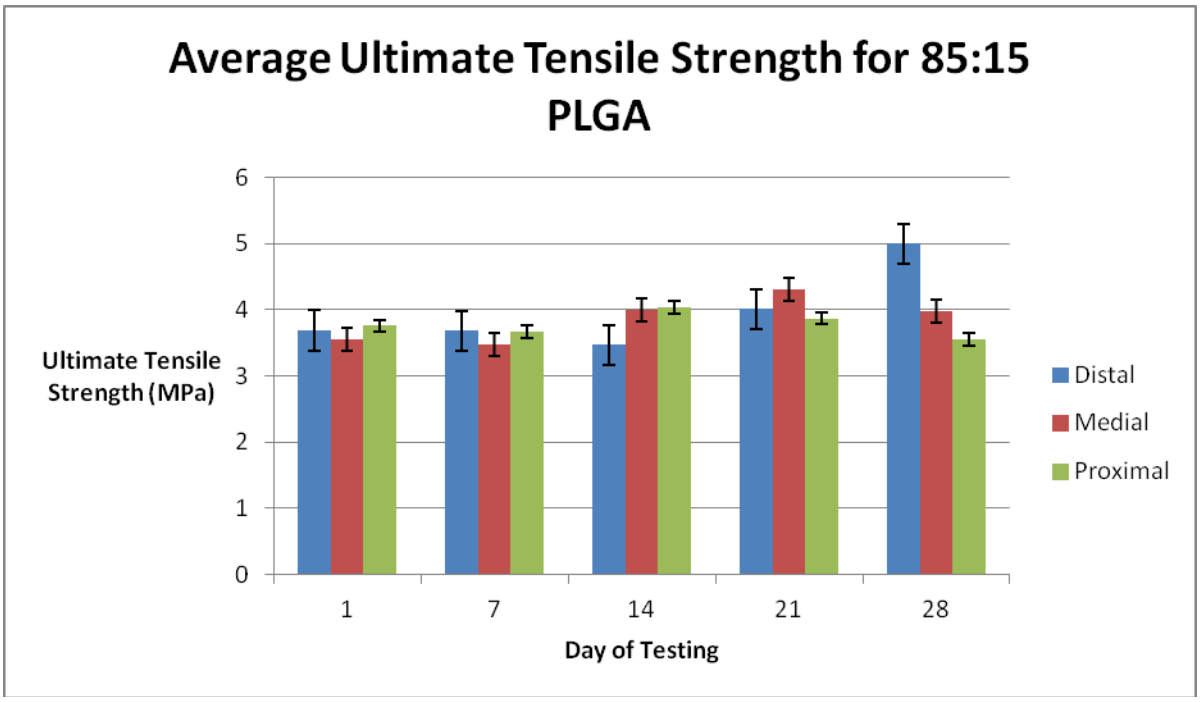

Figure 17: Average ultimate tensile strength for 85:15 PLGA for the distal, medial, and proximal regions of the scaffold over the course of 28 days; n = 4

When performing two-sample t-tests in Minitab, statistical differences were found in the medial region for days 7, 14, 21, and 28 compared to day 1 for 75:25 PLGA in terms of UTS. An increasing trend can be seen for all regions for 75:25 in figure 16. For 85:15 PLGA, there were no statistical differences found among the regions and the different days of testing in terms of UTS nor were there any major trends as can be seen in figure 17.

IV. Discussion

The goal of our project was to investigate if the morphology and mechanical properties of the scaffolds change over time when they are stored in the dessicator, and to set time points to note any statistically significant changes in fiber morphology and mechanical properties. In addition, 75:25 and 85:15 PLGA copolymers were compared in terms of fiber diameter, elastic modulus, and critical yield strength. These same three parameters were analyzed for the distal, medial, and proximal regions of the scaffold for each concentration.

In terms of fiber morphology, it seems that the 75:25 scaffolds have less overlapping fibers and are more consistent overall. Further study must be done to quantify porosity. In terms of fiber diameter, no significant differences were found among the regions of the scaffold for 75:25 or 85:15 PLGA, meaning that fiber diameter is relatively consistent along the length of the scaffold. There were also no significant changes over the course of the study, which was expected as long as moisture was removed from the scaffolds to prevent swelling in the dessicator. It was expected that fiber diameter should be greater for 75:25 PLGA compared to 85:15 PLGA because PGA has a greater molecular weight than PLA. As the molecular weight of the polymer or the polymer concentration is increased, so too does the solution viscosity. This, in turn, causes the formation of larger diameter fibers which lend improved mechanical properties, especially tensile strength to the scaffold [22]. However, this was not the case as no significant differences existed between the concentrations in terms of fiber diameter; in fact, 85:15 PLGA was slightly higher on average. This may be attributed to the fact that a slightly higher voltage was used (12.5 kV instead of 12.0 kV) when electrospinning the 85:15 scaffolds, which would then produce smaller diameter fibers than expected.

In terms of elastic modulus, a significant decrease in modulus was noted after day 7 for 85:15 PLGA but not for 75:25. There were significant differences between the concentrations after day 7 as well, since the modulus for 85:15 dropped dramatically. There were no differences among the regions of the scaffold for either concentration. In terms of UTS, there was a significant increase after day 1 for 75:25 but not for 85:15. Once again, there were no differences among the regions of the scaffold for either concentration nor were there significant differences between the concentrations. Modulus and yield strength were expected to be higher for the 75:25 samples because the crystallinity of PGA is higher than for PLA. As crystallinity increases, the

mechanical and thermal properties of the polymer such as strength tend to increase [21]. This theory seems to be true for modulus, which was significantly higher for 75:25 but may not necessarily be true for UTS. Although, UTS did steadily increase for 75:25 over the course of the study while it remained relatively level for 85:15, meaning that if the study was carried out longer, significant differences may have been found between the two concentrations in terms of UTS.

When comparing the values of the Elastic Modulus, UTS, and fiber diameter of this study to Tiffany Peña, the majority of the results from both studies are very similar, besides elastic modulus. Table 2 below compares the results of this study and Tiffany's.

Table 2: Comparison between Studies

	Elastic Modulus (MPa)	UTS (MPa)	Fiber Diameter (μm)
Tiffany	39.4	4.29	5.49
Sean/Nick	19.45	3.46	6.97

It is important to note the difference in parameters used to electrospin when comparing results for the two studies. The first is the orientation of the sample. Both of the studies tested samples in a circumferential orientation. Both studies also used a flow rate of 5.5 mL per hour. The parameter that was changed between the two studies was the applied voltage. This study used a slightly higher voltage of 12.5 kV as compared to 12 kV in Tiffany's study. However, it is unlikely that this small change in voltage would be enough to cause such a great change in the elastic modulus. It is more likely the difference in cutting procedures for the scaffolds that induced such a great change. This will be discussed more in the next section. Additionally, with a larger sample size used in this study, mandrels needed to be modified to allow for higher

throughput. Specifically, a special attachment was used on some of the newly created mandrels, which is pictured in figure 18 below.

Figure 18: Attachment for the mandrel to fit into the collector system properly (pictured on the left side of the mandrel)

It is possible that this attachment may have skewed some of the results in terms of how the fibers aligned and may have stretched the scaffold when removing it from the mandrel, but from our previous study (Appendix A4) it seems that the data we are getting is still consistent and not significantly affected by this attachment.

V. Limitations

Our current procedure includes sectioning the scaffold by cutting it with a razor blade. This method causes slight variations in the fiber morphology at the edges of samples and can create stress concentrations in the sample. These stress concentrations may cause variations in the sample's mechanical properties. With our current tensile testing fixture, this is unavoidable. Samples must be cut into strips so that they can be loaded into the tensile tester. Furthermore, variations in tensile testing technique will yield inconsistent results. Loading samples into the tensile tester changed the overall shape of the sample, which may cause changes in the fibers. We notice that by flattening the samples when placing them into the test fixtures, a crease formed in the sample. Failure in the samples consistently occurred along this crease. This crease

may have caused premature failure in our samples. Additionally, during the later testing days, samples became more difficult to load into the tensile tester. For the first fourteen days of SEM testing, the SEM was not properly calibrated, producing low quality images that made fiber analysis very difficult in ImageJ.

VI. Future Work

Future iterations of this study should use a different test fixture. To avoid variations in data, the scaffold itself should be intact. There is an existing test fixture that would allow testing of tubular samples. By not deforming a sample through sectioning, more consistent and accurate data can be obtained. Further work in electrospinning should include a study to optimize electrospinning parameters for the 85:15 PLGA concentration. To further characterize the scaffold, porosity should be quantified for each scaffold. This is one of the more important properties of scaffolds that influence cell seeding and adhesion.

VII. Conclusions

From our study, it can be concluded that mechanical properties and fiber morphology do not change along the scaffold length, at least in terms of the parameters tested. 75:25 PLGA seems to be a better concentration to use for BVM studies based on SEM images taken and slightly improved mechanical properties exhibited, although this is merely based on trends. A longer and larger study would be needed to validate this claim. Lastly, although there were no major changes in scaffold properties that would deem them to be “unusable” over the course of this study, we still recommend using the PLGA scaffolds within two weeks as noted by significant changes in mechanical properties at day 14 for both concentrations.

VIII. References

1 "Atherosclerosis." *New Medical Information and Health Information (NMIHI)*.

2 "What Is Atherosclerosis?" *National Heart Lung and Blood Institute*. U.S. Department of Health & Human Services, 1 July 2011.

3 "Atherosclerosis." *HealthCentral*. Remedy Health Media.

4 "Arteriosclerosis / Atherosclerosis." *Mayo Clinic*. Mayo Foundation for Medical Education and Research, 27 June 2012.

5 "Minimally Invasive Heart Bypass Surgery." *Cardiothoracic Surgery*. University of California Keck School of Medicine.

6 Image: http://americaninvetors.blogspot.com/2009/05/coronary-artery-bypass-surgery.html

7 "Tissue Engineering." *Science*. <http://www.sciencemag.org/content/260/5110/920>.

8 Jennifer Elisseeff; Peter X. Ma (2005). Scaffolding In Tissue Engineering. Boca Raton: CRC.

9 Leifer, Sara M. "Design and Optimization of a Blood Vessel Mimic Bioreactor System for the Evaluation of Intravascular Devices in Simple and Complex Vessel Geometries." (2008).

10 Image: http://www.ctecohio.org/projects_bioreactors/project14_bioreactors.htm

11 Huang, Zheng-Ming, et al. "A review on polymer nanofibers by electrospinning and their applications in nanocomposites." Composites science and technology 63.15 (2003): 2223-2253.

12 Tsing, P. (2007). Electrospinning Natural Polymers for Tissue Engineering Applications. University of Pennsylvania.

13 Liang, Dehai, Benjamin S. Hsiao, and Benjamin Chu. *"Functional electrospun nanofibrous scaffolds for biomedical applications."* Advanced drug delivery reviews 59.14 (2007): 1392-1412.

14 "Electrospinning." Electrospinz. N.p., n.d. Web. 10 Dec. 2012. <http://www.electrospinz.co.nz/electrospinning.php>.

15 Lu, Ping, and Bin Ding. "Applications of Electrospun Fibers." *Recent Patents on Nanotechnology* 2 (2008): 169-82. ResearchGate, 30 June 2008.

16 Liu, Xiaohua, and Peter X. Ma. "Polymeric Scaffolds for Bone Tissue Engineering: on Musculoskeletal Bioengineering. Guest Editor: Kyriacos A. Athanasiou." Annals of biomedical engineering 32.3 (2004): 477-486.

17 "Poly(lactic Acid) and Poly(glycolic Acid) and Their Copolymers." Freedownloadb.com, 2011. <http://freedownloadb.com/doc/polylactic-acid-and-polyglycolic-acid-and-their-copolymers-2427771.html>.

18 "Electrospinning." <http://www.che.vt.edu/Wilkes/electrospinning/electrspinning.html>.

19 James, C. M. "Assessment of Electrospinning as an In-House Fabrication Technique for Blood Vessel Mimic Cellular Scaffolding." *Master's Theses and Project Reports* (2009): 185.

20 Ramakrishna, Seeram. An Introduction to Electrospinning And Nanofibers. Singapore: World Scientific, 2005.

21 Walsh, Dan. Class Lecture. Biomaterials. California Polytechnic State University, San Luis Obispo, CA. 5 February 2013.

22 Lalani, Reza, and Lingyun Liu. "Synthesis, characterization, and electrospinning of zwitterionic poly (sulfobetaine methacrylate)." Polymer 52.23 (2011): 5344-5354.

23 "Heart Disease Facts and Statistics." Centers for Disease Control and Prevention, 16 Oct. 2012. Web. <http://www.cdc.gov/heartdisease/statistics.htm>.

24 Makadia, Hirenkumar K., and Steven J. Siegel. "Poly Lactic-co-Glycolic Acid (PLGA) as Biodegradable Controlled Drug Delivery Carrier." *Polymers* 3.3 (2011): 1377-397. Web. 5 Aug. 2013.

25 Pena, Tiffany Richelle. "Preparation and Characterization of Electrospun Poly (D, L-lactide-co-glycolide) Scaffolds for Vascular Tissue Engineering and the Advancement of an In Vitro Blood Vessel Mimic." *Master's Theses and Project Reports* (2009): 152.

26 Patel, Deven. "Preparation and characterization of electrospun poly (D, L-Lactide-co-Glycolide) scaffolds for vascular tissue engineering and the advancement of an in vitro blood brain barrier model." *Master's Theses and Project Reports* (2012): 824

IX. Appendix

A1: Mixing PLGA Solutions

*Note: Protocol used comes from Tiffany R. Pena's thesis.

Table 1: Bill of Materials

Materials/Equipment	Vendor	Part Number	Quantity
Poly (DL-lactide-co-glycolide) (PLGA) Lactide: Glycolide (75:25) Mol wt 66,000 - 107,000	Sigma-Aldrich	P1941	5 grams
Chloroform, extra dry, water <50ppm, stabilized	Fisher Scientific, Inc	326820010	1 Liter
10 ml Syringe, Luer-Lok tip	BD	309604	100/Pack
Blunt Fill Needle, 18G 1 ½ (1.2 mm x 40 mm)	BD	305180	100/Pack
Analytical Balance	Acculab	ALC-80.4	1
Orbital Shaker [check new shaker]			1
Vacuum-Pressure Pipette Aid	Drummon Scientific Co.	P-80991	1
Serological Pipet 5 x 1/10 ml	VWR International	53283-706	NA
Clear Glass Vial 20 ml	VWR International	15900-002	72/CS

Procedure

1. Calculate the amount of PLGA resin necessary for the desired weight percent polymer solution using the following equation. (Density of chloroform is 1.48 g/ml.)

$$WPP = m1/ (m1 + m2b)$$

*WPP = Weight percent polymer solution

m1 = mass of polymer (g)

m2 = mass of solvent (ml)

b = density of solvent (g/ml)

$$.15 = \frac{m_1}{m_1 + m_2 b}$$

$$m_1 = .15m_1 + .15(3\,ml)\left(1.48\frac{g}{ml}\right)$$

$$**m_1 = 0.7835294118\,g$$

*Always use 0.15 for WPP

**Mass of polymer for a 3mm scaffold

Note: For 4mm scaffold, use 1.0447 g.

2. Put on safety gloves. (*WARNING: Chloroform can have serious side-effects if it comes in contact with skin, eyes or is inhaled or swallowed. Target organs to be effected are kidneys, heart, central nervous system, liver, eyes, reproductive system and skin. Always open chloroform in a hood and wear protective clothing!!*

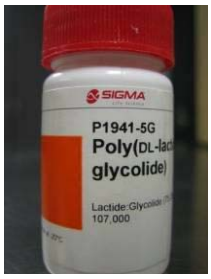

Figure 2: Bottled PLGA

3. Remove PLGA (Figure 2) from the freezer and allow it to reach room temperature (5-10 minutes). Doing so prevents condensation when the polymer is exposed to air.

Figure 3: Acculab Balance

4. Weigh out the calculated amount of PLGA using the Acculab Balance (**Error! Reference source not found.**) and place the polymer in a 20 ml clear vial. Close the lid immediately.
5. Return unused PLGA to the freezer.
6. Retrieve the chloroform (Figure 4) for the hazardous chemical cabinet and place it in the fume hood immediately.

Figure 4: Bottled chloroform

7. Gather the Pipette-Aid, a 10 ml disposable pipette and the vial of weighed PLGA and place in the hood with the chloroform.
8. Pipette the desired volume of chloroform into the vial with PLGA. Immediately cap the vial as well as the chloroform container to prevent evaporation of chloroform since it is highly volatile.

9. Properly label the solution vial with the WPP, date and your initials (Figure 5).
10. Wrap vial in aluminum foil to prevent light from entering the solution (chloroform is highly sensitive to light).
11. Place the vial on the shake table. Set the shake table to approximately 3 revolutions per second. Use tape to ensure that the vial will stay upright while on the shake table. Turn the table on.

Figure 5: Labeled vial of WPP

12. Allow the solution to mix for 24 hours. After mixing is complete, the solution is usable for up to 48 hours.
13. Remove chloroform container from hood and place back into chemical cabinet.
14. Properly dispose of the pipette tip.
15. Clean up work area.

A2: Electrospinning Protocol

*Protocol is a modified version of Deven Patel's protocol for electrospinning.

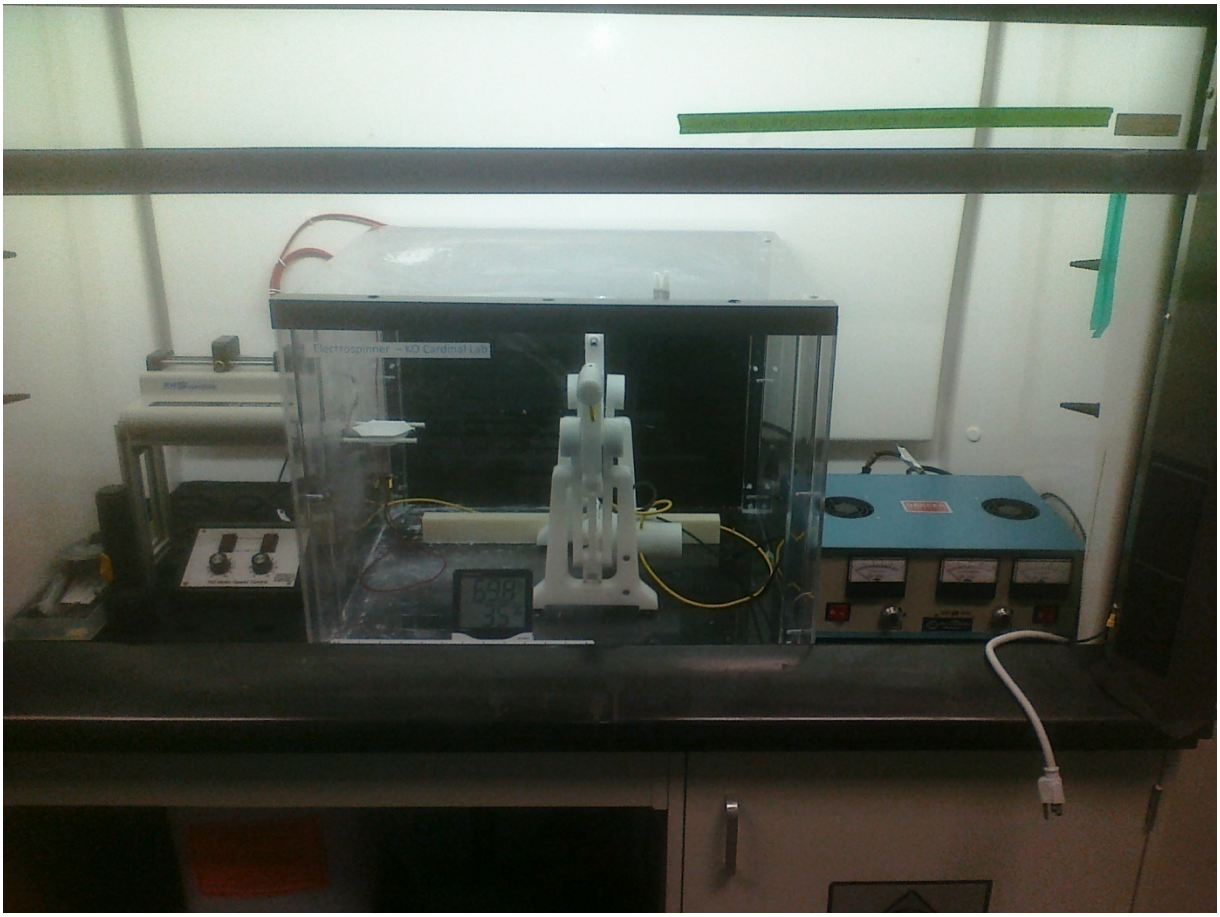

<u>WARNING:</u> This process utilizes extremely high voltages. Always wear shoes, gloves, and be careful of what you are contacting. To use the electrospinner, you must be trained by a qualified user and be approved by an appropriate faculty member.

<u>Polymer:</u>	15wt% PLGA in Chloroform ($CHCl_3$)
<u>Flow Rate:</u>	5.5ml/hr, 3ml of polymer solution used
<u>Needle:</u>	18 gauge, beveled, blunt (BD 305180)
<u>Gap:</u>	10 inches
<u>Voltage:</u>	- 12,500V (negative polarity)
<u>Translate:</u>	Distance set at 10 in., translation speed set at 3 or 55 OPM
<u>Rotate:</u>	Rotation speed at 6 or 3110 RPM

1) Put on latex gloves.
2) Clean debris left from previous spins using paper towels and isopropal alcohol (IPA). Be sure to clean polymer collection system (Figure 1) and inside walls of the isolation chamber.
3) Sand mandrel with 1200 grain sandpaper (Figure 2), then spray and clean off with IPA. Be sure that the mandrel is clean before using it.
4) Insert mandrel into collector.
5) Attach an 18 gauge BD needle to a BD 10ml plastic syringe.
6) Inside the fume hood, pull the desired amount of polymer solution into the syringe. The polymer solution is very viscous, so this will take some time. Be sure that there is no air within the syringe. Use a wipe to purge the air from the syringe.
7) Place needle through the small hole drilled in the isolation chamber and set the syringe onto the syringe pump (Figure 3).
8) Secure the syringe into position using the black clamp on the syringe pump.
9) Clip the red high voltage alligator clip to the needle inside the isolation chamber, see Figure 4.
10) Position the collection system in the isolation chamber so

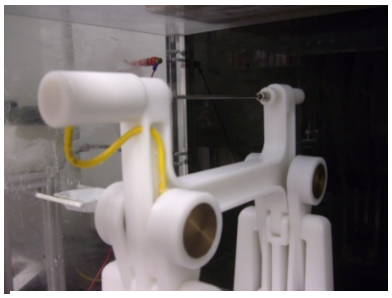

Figure 1: Clean collection system

Figure 2: Sand mandrel with sand paper

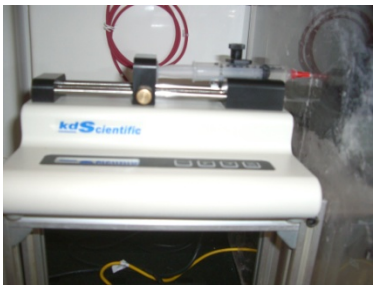

Figure 3: Secure syringe on syringe pump, and place needle into the isolation chamber

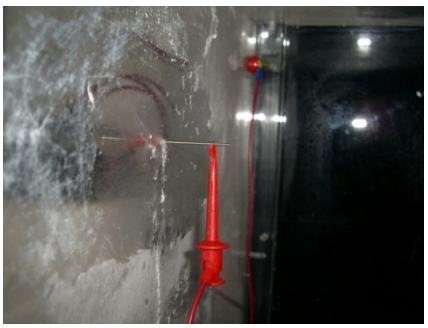

Figure 4: Attach high voltage alligator clip to needle.

that the metal mandrel and needle tip are at the desired gap distance and perpendicular to each other

11) Take the black ground banana plug and connect to the collector system as seen in Figure 5.

Figure 5: Connect black ground wire to collection system.

12) Using a multimeter, check the resistance between the ground connection and the aluminum mandrel to verify conductivity. One should see very little resistance (fractions of an ohm) if the mandrel is properly grounded. If a very high resistance is detected, the mandrel is no longer maintaining continuity with the ground wire.
13) Close the front panel of the isolation chamber.
14) Next, plug in the surge protector into the wall outlet of the fume hood.
15) Flip the green switch on the surge protector to turn it on, and as a result provide power to the syringe pump, rotation and translation regulator, and power supply.
16) Switch on the syringe pump, and enter the desired settings (syringe type, volume, flow rate, etc.). The syringe pump will maintain the same settings that were used previously. So if no one has used the apparatus since, there is no need to make any changes to the syringe pump programming.

    Syringe Type: BD 10 ml Plastic syringe (select from syringe pump library)
    Volume: 3 mL
    Flow Rate:5.5 ml/hr

Figure 6: High Voltage Power supply.

17) Turn on the "Rotate" and "Slide" functions of the collector at the regulator box. The speed at which the mandrel rotates and translates is controlled from this box. Settings 3 for translation, and 6 for rotate.
18) Press the "Run" button on the syringe pump so that the polymer solution will begin ejecting at a controlled volumetric rate.

19) Once a polymer droplet forms at the tip of the spinneret, the electrospinning process is ready to start. Immediately turn on the power supply (Figure 6), press red button, and adjust output voltage knob to the desired applied voltage.
20) Observe the process of the entire spin, slowly the metal mandrel will become visibly coated with polymer (white color).
21) Once the desired amount of polymer solution has been electrospun, the process should be shut down in the following manner.

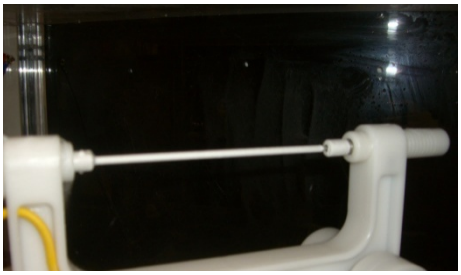

Figure 7: Detach polymer coated mandrel from collection system

22) Turn the high voltage power supply off, by flipping the red switch to "off."
23) Next, press the "Run/Stop" button on the syringe pump to stop the pump. Then turn the syringe pump off.
24) Turn the "Rotate" and "slide" switches off on the regulator box.
25) Flip the green switch of the surge protector to "off." And then unplug the surge protector from the wall outlet of the fume hood.
26) Slide open the front panel of the isolation chamber and wait for a few minutes to allow the evaporated solvent to leak out and be taken up by the fume hood.
27) Detach the polymer coated mandrel from the collector system, see Figure 7.
28) Contact the red high voltage alligator clip to the black ground wire to remove any residual charge.
29) Clean any polymer fiber debris using paper towels and isopropal alcohol (IPA). Be sure to clean polymer collection system (Figure 1) and inside walls of the isolation chamber.

Figure 8: Dispose any material that came in contact with chloroform into Hazardous Waste bucket.

30) Dispose of the syringe needle in the sharps container.
31) Dispose syringe and polymer solution vials into Hazardous Waste bucket, Figure 8.
32) Take the polymer coated mandrel to the desiccator and leave for at least 24 hours before sectioning, Figure 9.
33) Cut polymer scaffold off of metal mandrel between 24-48 hours later (once polymer is completely dry) and place onto glass rod in desiccator; be sure rod is labeled clearly (with tape).
34) Return metal mandrel to top of desiccator box.

Figure 9: Place metal mandrel with polymer scaffold around it into the desiccator after electrospinning.

A3: Visual Basic Macro

*Note: Macro provided by Aubrey Dyer; later modified for our own study

```
Sub TensileTestMacro()
'December 12, 2012'
Dim Filename()
Close #1
k = 0
d = InputBox("How many tests would you like to analyze?")
If d > 3 Then
   For k = 4 To d        'you didn't type in a number'
Worksheets.Add
   Next
End If
For j = 1 To d
   m = 0
   Max = 0
sumofx = 0
sumofy = 0
sumofxy = 0
sumofxx = 0
sumofxsquared = 0
   Delta = 0
   a = 0
   b = 0
   c = 0
   l = 0
' Filename = InputBox("Enter the file", , "85_15_#1_d.csv")
' Pathname = InputBox("Enter the path to " + Filename, , "C:\Users\Public\Documents\Electrospinning\")
   Call FileDialogOpen(Filename())
myfile = Filename(j)
   Name = InputBox("What test is this?")
   a = InputBox("What is the gauge of the sample?")
   b = InputBox("What is the width of the sample?")
   c = InputBox("What is the thickness of the sample?")
Worksheets(j).Name = Name                    'you kept hitting cancel didn't you?'
Worksheets(Name).Cells(1, 1).Value = "Time"
Worksheets(Name).Cells(1, 2).Value = "Extension"
Worksheets(Name).Cells(1, 3).Value = "Load"
Worksheets(Name).Cells(1, 4).Value = "Strain"
Worksheets(Name).Cells(1, 5).Value = "Stress"
Worksheets(Name).Cells(1, 7).Value = "Linear Strain"
Worksheets(Name).Cells(1, 8).Value = "Linear Stress"
Worksheets(Name).Cells(1, 10).Value = "Critical/Yield Stress"
```

```
Worksheets(Name).Cells(1, 11).Value = "20% Yield Stress"
Worksheets(Name).Cells(1, 12).Value = "50% Yield Stress"
Worksheets(Name).Cells(1, 13).Value = "Slope"
Worksheets(Name).Cells(1, 14).Value = "y-intercept"
      Open myfile For Input As #j   'Typed the filename wrong/file doesn't exist/you've already opened it
this session'
i = 0
         Do Until EOF(j)
         Input #j, tm, x, y
            If i = 0 Ori = 1 Then
Worksheets(Name).Cells(i + 2, 1).Value = tm
Worksheets(Name).Cells(i + 2, 2).Value = x
Worksheets(Name).Cells(i + 2, 3).Value = y
i = 1 + i
            Else

            If (x >= 0) And (y > 0) Then
i = i + 1
Worksheets(Name).Cells(i - 1, 1).Value = i - 2            'need to delete the
Worksheets(Name).Cells(i - 1, 2).Value = x              'first two lines of
Worksheets(Name).Cells(i - 1, 3).Value = y              'the notepad file
Worksheets(Name).Cells(i - 1, 4).Value = x / a          '(only data points
Worksheets(Name).Cells(i - 1, 5).Value = y / (b * c)      'no words) or you messed up typing a value into
the size of the sample
               t = x / a
               u = y / (b * c)
               If u > Max Then
                  Max = u
timestop = (i - 2)
               End If
Worksheets(Name).Cells(2, 10).Value = Max
               e = (0.2) * Max
               f = (0.5) * Max
Worksheets(Name).Cells(2, 11).Value = e
Worksheets(Name).Cells(2, 12).Value = f
            End If
            End If
         Loop
      g = 0
      r = 0
      p = 1
      For m = 1 To (i - 2)
         g = g + 1
         o = Worksheets(Name).Cells(g, 1).Value
```

```
        h = Worksheets(Name).Cells(g, 5).Value
        n = Worksheets(Name).Cells(g, 4).Value

        If h >= e And h <= f And o <= timestop Then

          p = p + 1

Worksheets(Name).Select
Cells(g, 4).Select
Selection.Font.Bold = True
Cells(g, 5).Select
Selection.Font.Bold = True

Worksheets(Name).Cells(p, 7).Value = n
Worksheets(Name).Cells(p, 8).Value = h

          End If
      Next

Worksheets(Name).Cells(8, 1).Select

Charts.Add
   With ActiveChart
      .ChartType = xlXYScatterSmoothNoMarkers
      .SetSourceData Source:=Sheets(Name).Range("D:E"), PlotBy:=xlColumns
      .Location Where:=xlLocationAsObject, Name:=Name
   End With
   With ActiveChart
      .HasTitle = True
      .ChartTitle.Text = "Stress-Strain Curve"
      .Axes(xlCategory, xlPrimary).HasTitle = True
      .Axes(xlCategory, xlPrimary).AxisTitle.Characters.Text = "Strain"
      .Axes(xlValue, xlPrimary).HasTitle = True
      .Axes(xlValue, xlPrimary).AxisTitle.Characters.Text = "Stress"
      .HasLegend = False
   End With

Worksheets(Name).Cells(16, 6).Select
   q = p - 1

Charts.Add
   With ActiveChart
      .ChartType = xlXYScatter
      .SetSourceData Source:=Sheets(Name).Range("G:H"), PlotBy:=xlColumns
```

```
        .Location Where:=xlLocationAsObject, Name:=Name
    End With
    With ActiveChart
        .HasTitle = True
        .ChartTitle.Text = "Linear Stress"
        .Axes(xlCategory, xlPrimary).HasTitle = True
        .Axes(xlCategory, xlPrimary).AxisTitle.Characters.Text = "Strain"
        .Axes(xlValue, xlPrimary).HasTitle = True
        .Axes(xlValue, xlPrimary).AxisTitle.Characters.Text = "Stress"
        .HasLegend = False
    End With
ActiveChart.SeriesCollection(1).Select
'ActiveChart.SeriesCollection(1).Points(q).Select
ActiveChart.SeriesCollection(1).Trendlines.Add(Type:=xlLinear, Forward:=0, _
    Backward:=0, DisplayEquation:=True, DisplayRSquared:=True).Select
    Close #j
Next
End Sub


Sub FileDialogOpen(Filename())

    Dim lngCount As Long  ' allow for multiple file selection (Completely Optional!)

' Open the file dialog
    With Application.FileDialog(msoFileDialogOpen)
        .AllowMultiSelect = True   'This code is multiple file
        .Show
        n = .SelectedItems.Count
ReDimFilename(n)
' Display paths of each file selected

        For lngCount = 1 To n
Filename(lngCount) = .SelectedItems(lngCount)
        Next lngCount

    End With

End Sub
```

A4: Previous Study of 50:50 and 85:15 PLGA

Objective:

To determine if varying the concentrations of PLA and PGA that make up the copolymer PLGA affect the resulting fiber characteristics and mechanical properties. In addition, the effect of the local environment will be investigated in terms of if the properties change in a "wet" vs. "dry" environment.

Methods:

The two concentrations that were tested were 50:50 and 85:15 PLGA. Four scaffolds of the 50:50 and four scaffolds of the 85:15 were electrospun using a flow rate of 5.5 ml/hr and a voltage of 13.5 kV. All eight scaffolds were spun on the same day. In order to accomplish this, six mandrels had to be created that were 0.118 inches in diameter instead of the usual 0.125 inches. The two pre-made mandrels that were readily available had a diameter of 0.125 inches. After a 24-hour waiting period, each of the scaffolds was sectioned so that each 1 cm sample would be used for tensile testing and each 0.5 cm sample would be used for SEM image analysis. The samples were separated into 6-well plates and each well was labeled according to the test day, the type of test, concentration of the copolymer, and whether the sample was soaked in Medium 199 or not ("wet" vs. "dry"). The samples that were soaked in the media were placed in the fridge in centrifuge tubes until the day of testing. Testing was done every 7 days, starting with day 1 which occurred 24 hours after sectioning the samples. Day 1, 7, and 14 had wet and dry sample testing, while day 21 and 28 only had dry testing. For SEM analysis, the samples had to be dehydrated one day prior to testing. For each day of testing, three tests were conducted for each concentration to allow for statistical analysis and comparison of the data later on.

Results:

SEM images were taken for all wet and dry samples for both concentrations on the particular day of testing. All images were taken at 500x magnification as specified in the methods section. Representative images for the two concentrations, 50:50 and 85:15 PLGA, are shown below in figures 1 and 2, for wet and dry samples respectively.

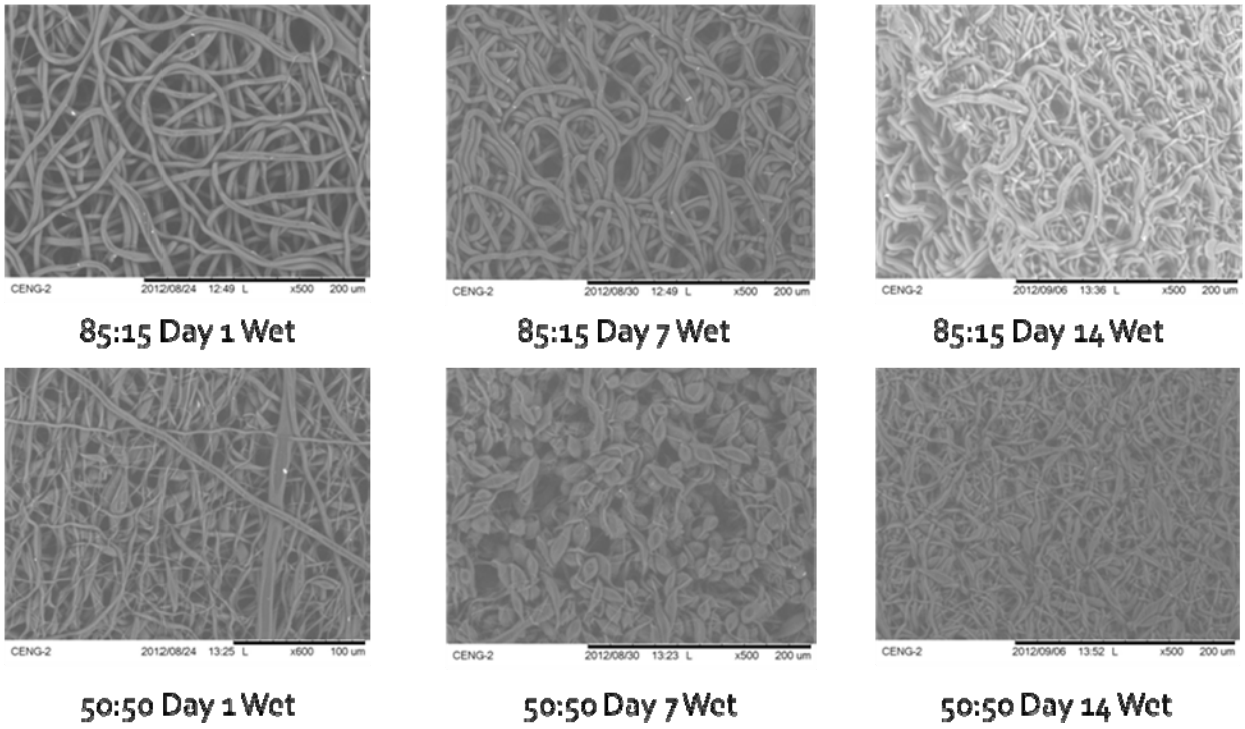

Figure 1: Representative SEM images for 85:15 and 50:50 PLGA wet samples over the course of 14 days

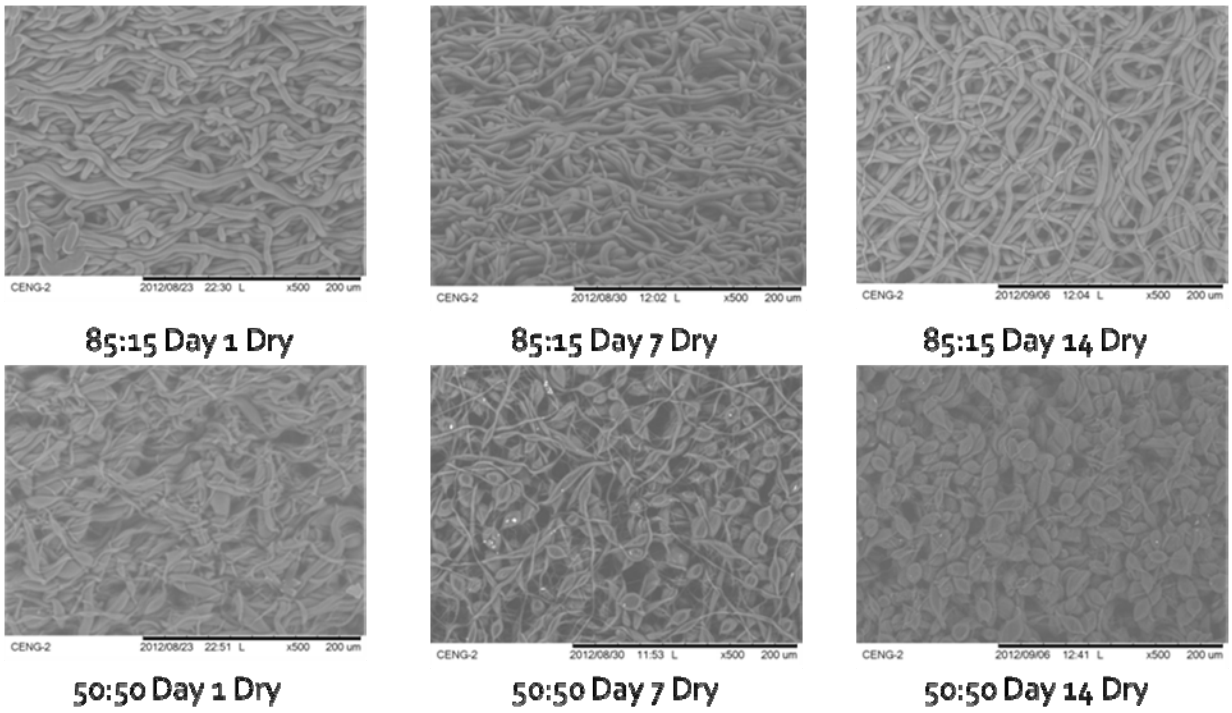

Figure 2: Representative SEM images for 85:15 and 50:50 PLGA dry samples over the course of 14 days

Important things to note about the images include the relative porosities, alignment of the fibers, thickness of the fibers, and overall consistency of the fibers. After all images had been taken for a particular day of testing, 6 fibers were analyzed in ImageJ for each image and an average was taken. A comparison of average fiber diameters of wet and dry samples for 85:15 PLGA over the course of 14 days can be seen in figure 3, in which dry samples were significantly different from wet samples.

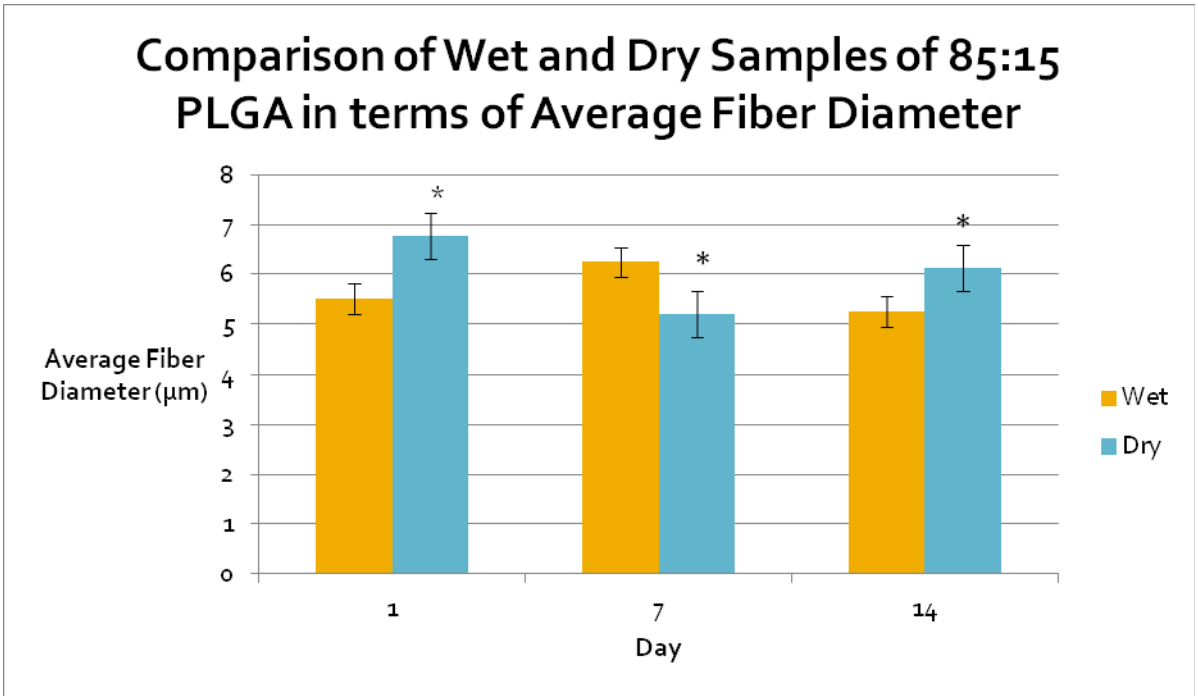

Figure 3: Wet and dry samples of 85:15 PLGA in terms of average fiber diameter over the course of 14 days; n = 3; *, $p < 0.05$

The average fiber diameters from different days of testing were also compared to day 1 to distinguish if there were any trends. Figure 4 shows this progression for wet samples while figure 5 shows the same for dry samples. There was only a significant difference at day 14 for wet samples. After day 1, the fiber diameter continued to change significantly for dry samples.

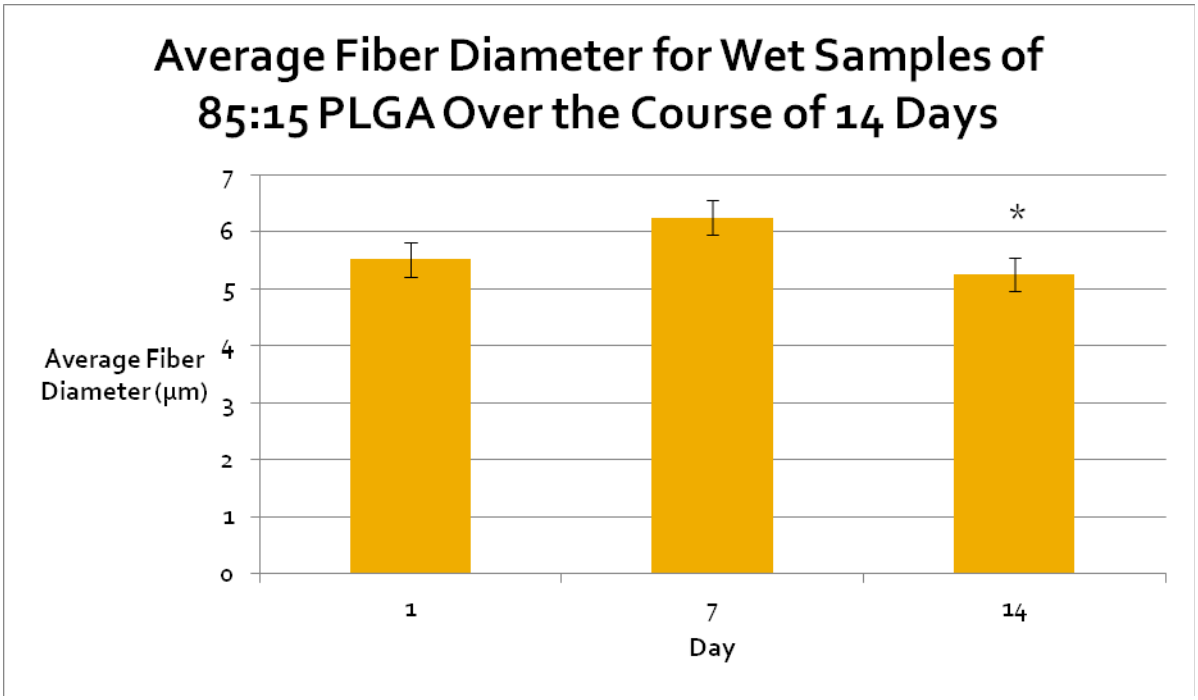

Figure 4: Wet samples of 85:15 PLGA in terms of average fiber diameter over the course of 14 days; n = 3; *, $p < 0.05$ versus day 7

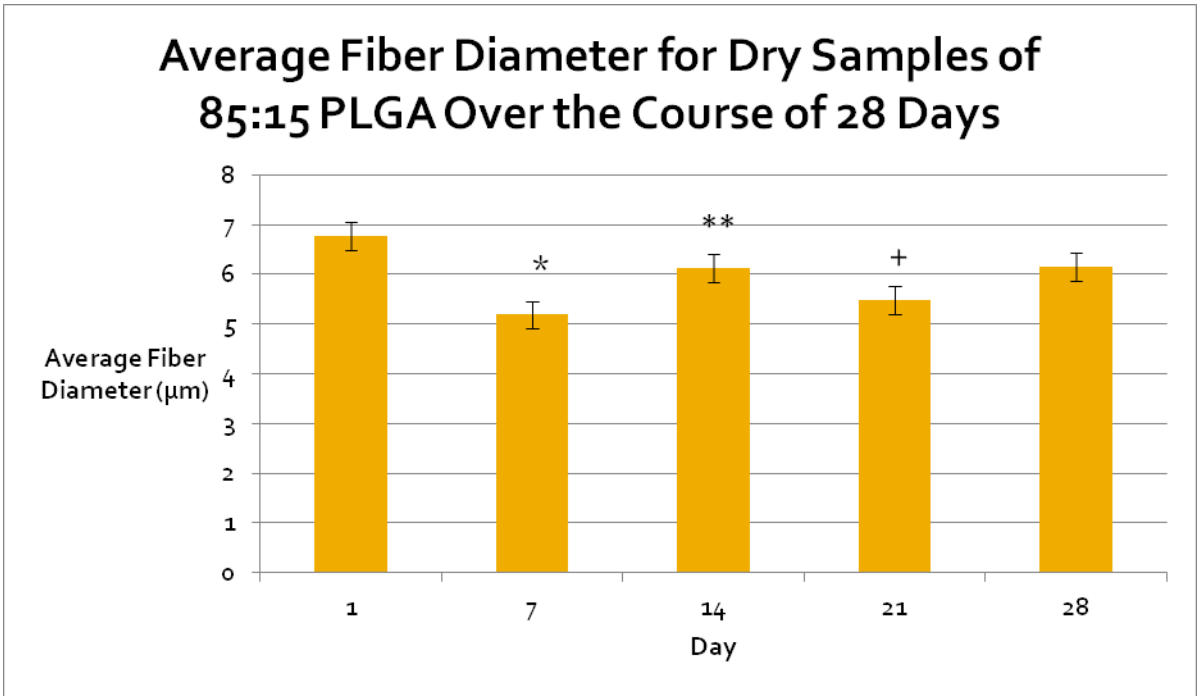

Figure 5: Dry samples of 85:15 PLGA in terms of average fiber diameter over the course of 28 days; n = 3; *, $p < 0.05$ versus day 1; **, $p < 0.05$ versus day 7; +, $p < 0.05$ versus day 1

Tensile testing was performed and stress-strain curves were outputted using the macro found in appendix A3. Representative stress-strain curves for 85:15 PLGA dry samples are shown in figure 6. A side-by-side comparison of both wet and dry stress-strain curves for 85:15 PLGA is shown in figure 7.

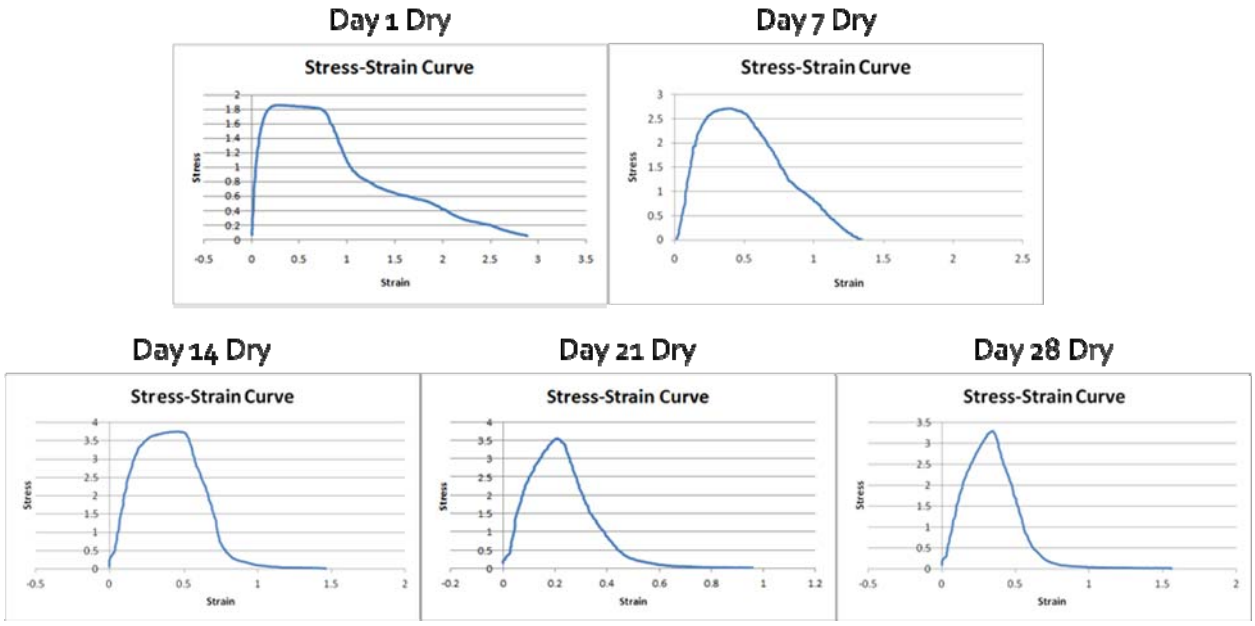

Figure 6: Representative stress-strain curves for 85:15 PLGA dry samples over the course of the study

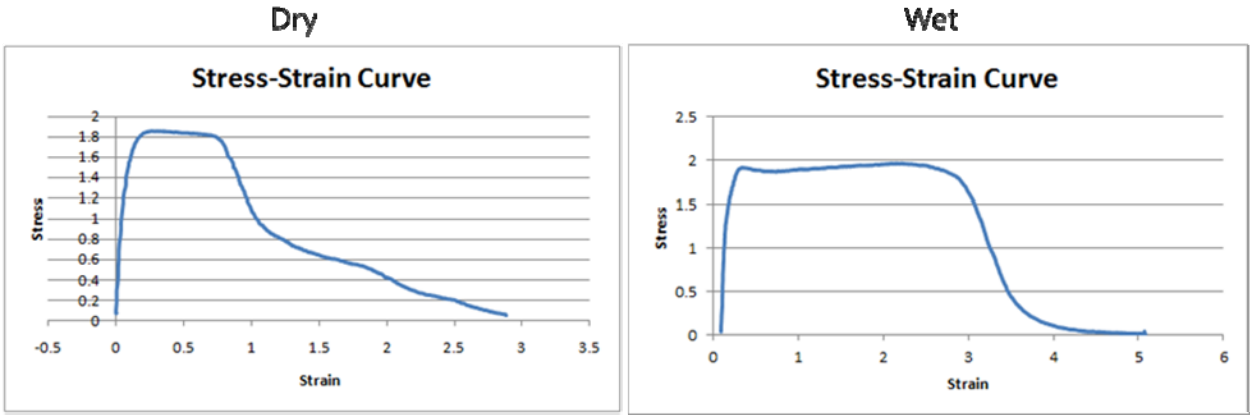

Figure 7: Representative stress-strain curves for 85:15 PLGA wet and dry samples

The linear portion of the stress-strain curve was also outputted simultaneously and the equation of the line provided the elastic modulus of the sample. In Excel, the ultimate tensile strength (UTS) was found from the maximum stress point along the curve and this was displayed as well. Average elastic modulus for 85:15 PLGA wet and dry samples over the course of the study can be seen in figure 8. Average UTS for 85:15 PLGA wet and dry samples over the course of the study can be seen in figure 9. No significant differences were found in terms of elastic modulus, but there were significant differences for UTS after day 7 of testing.

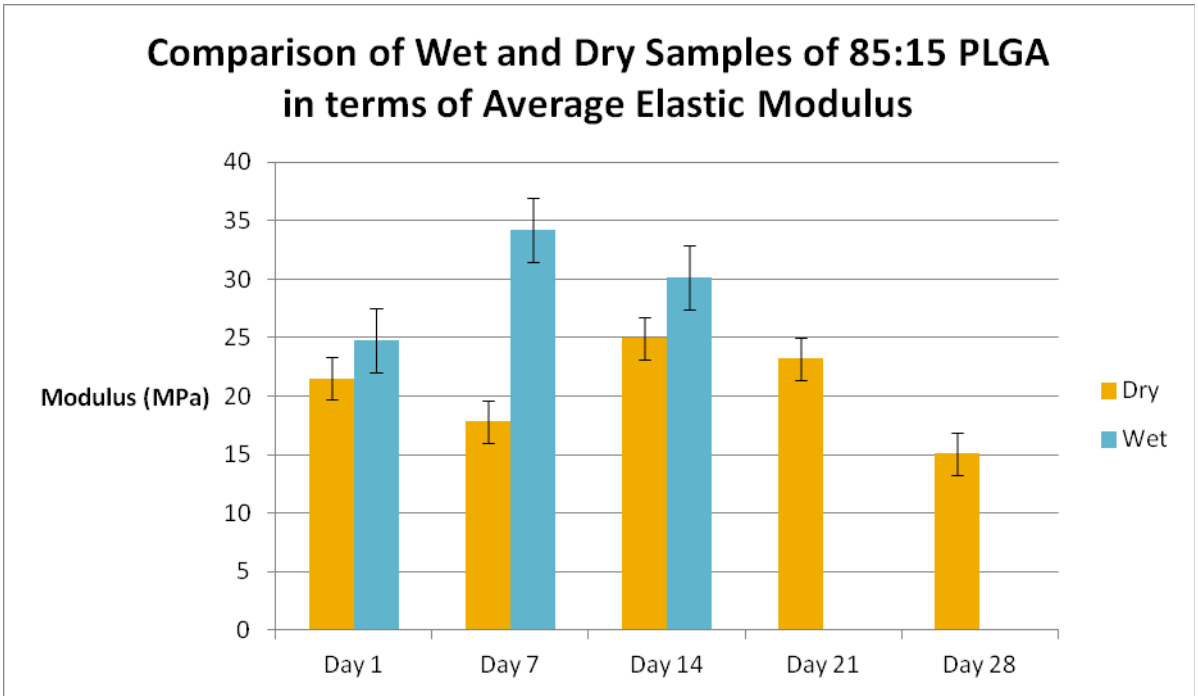

Figure 8: Wet and dry samples of 85:15 PLGA in terms of average elastic modulus over the course of 28 days; n = 3

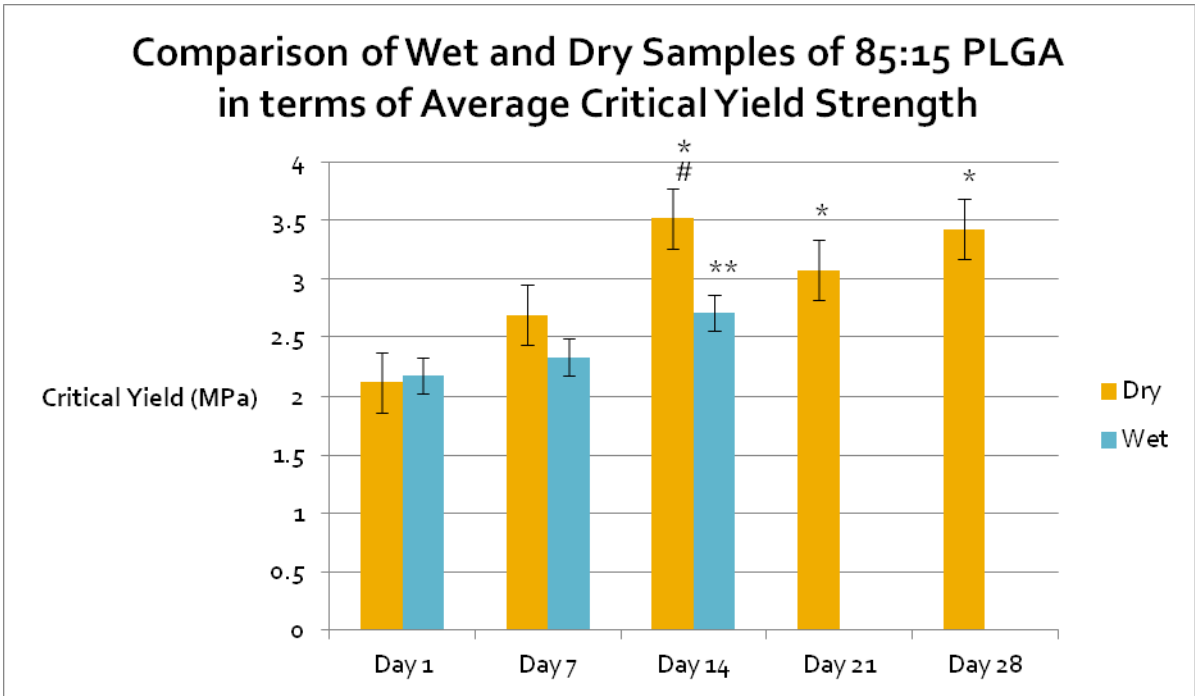

Figure 9: Wet and dry samples of 85:15 PLGA in terms of average critical yield strength over the course of 28 days; n = 3; *, p < 0.05 versus day 1; #, p < 0.05 versus day 7; ** p < 0.05 versus day 14 wet

Discussion:

The objective of this study was to determine if varying the concentrations of PLA and PGA that make up the copolymer PLGA affect the resulting fiber characteristics and mechanical properties, in which 50:50 and 85:15 PLGA were compared. In addition, the effect of the local environment was investigated in terms of if the properties change in a "wet" vs. "dry" environment by placing some of the samples in media and allowing them to soak before testing.

It cannot necessarily be stated that there is a definite increase or decrease in fiber diameter with time or between wet and dry samples, despite the statistical differences seen in figures 3, 4 and 5. The confidence level may actually be too high for such measurements and a smaller p-value may be needed to truly tell whether significant differences exist in this data. The stress-strain curves for the wet and dry samples are fairly similar, although the time to failure, in which plastic deformation is occurring, seems to be much greater for the wet samples. During the data

collection for tensile testing, we noticed that the 50:50 samples tore pre-maturely near the clamps and had very low yield strength compared to the 85:15 samples. Once we looked at the 50:50 samples under the SEM, we noticed beading had occurred in some of the samples instead of the more elongated fibers that are obviously more ideal. This beading led to very poor mechanical properties (modulus and yield strength) and would not be suitable as constructs for BVMs. This inconsistency in fiber diameter leads us to believe that the original parameters i.e. voltage and flow rate are not ideal for the 50:50 co-polymer and that further experimentation into optimizing these two parameters must be conducted in order to achieve consistent fibers as seen in the 85:15 samples.